

AD_____

Award Number: W81XWH-04-1-0843

TITLE: Fibroblast Growth Factor Receptor-4 and Prostate Cancer Progression

PRINCIPAL INVESTIGATOR: Michael M. Ittmann M.D.; Ph.D.

CONTRACTING ORGANIZATION: Baylor College of Medicine
Houston, Texas 77030

REPORT DATE: October 2007

TYPE OF REPORT: Final

PREPARED FOR: U.S. Army Medical Research and Materiel Command
Fort Detrick, Maryland 21702-5012

DISTRIBUTION STATEMENT: Approved for Public Release;
Distribution Unlimited

The views, opinions and/or findings contained in this report are those of the author(s) and should not be construed as an official Department of the Army position, policy or decision unless so designated by other documentation.

REPORT DOCUMENTATION PAGE

*Form Approved
OMB No. 0704-0188*

Public reporting burden for this collection of information is estimated to average 1 hour per response, including the time for reviewing instructions, searching existing data sources, gathering and maintaining the data needed, and completing and reviewing this collection of information. Send comments regarding this burden estimate or any other aspect of this collection of information, including suggestions for reducing this burden to Department of Defense, Washington Headquarters Services, Directorate for Information Operations and Reports (0704-0188), 1215 Jefferson Davis Highway, Suite 1204, Arlington, VA 22202-4302. Respondents should be aware that notwithstanding any other provision of law, no person shall be subject to any penalty for failing to comply with a collection of information if it does not display a currently valid OMB control number. **PLEASE DO NOT RETURN YOUR FORM TO THE ABOVE ADDRESS.**

1. REPORT DATE (DD-MM-YYYY) 01-10-2007			2. REPORT TYPE Final		3. DATES COVERED (From - To) 15 SEP 2004 - 14 SEP 2007	
4. TITLE AND SUBTITLE Fibroblast Growth Factor Receptor-4 and Prostate Cancer Progression			5a. CONTRACT NUMBER			
			5b. GRANT NUMBER W81XWH-04-1-0843			
			5c. PROGRAM ELEMENT NUMBER			
6. AUTHOR(S) Michael M. Ittmann M.D.; Ph.D. E-Mail: mittmann@bcm.tmc.edu			5d. PROJECT NUMBER			
			5e. TASK NUMBER			
			5f. WORK UNIT NUMBER			
7. PERFORMING ORGANIZATION NAME(S) AND ADDRESS(ES) Baylor College of Medicine Houston, Texas 77030			8. PERFORMING ORGANIZATION REPORT NUMBER			
9. SPONSORING / MONITORING AGENCY NAME(S) AND ADDRESS(ES) U.S. Army Medical Research and Materiel Command Fort Detrick, Maryland 21702-5012			10. SPONSOR/MONITOR'S ACRONYM(S)			
			11. SPONSOR/MONITOR'S REPORT NUMBER(S)			
12. DISTRIBUTION / AVAILABILITY STATEMENT Approved for Public Release; Distribution Unlimited						
13. SUPPLEMENTARY NOTES						
14. ABSTRACT We have found that the FGFR-4 Arg388 allele is strongly associated with the occurrence of prostate cancer and with metastasis and PSA recurrence in men undergoing radical prostatectomy. Our published data indicates that FGFR-4 plays an important role in prostate cancer initiation and progression. We have now proven that FGFR-4 plays an important role in prostate cancer progression <i>in vivo</i> . We have established that Ehm2 plays an important role in this process. Furthermore, HIP1 plays an important role in modulating FGFR-4 Gly388 activity and is associated with more aggressive prostate cancer.						
15. SUBJECT TERMS Fibroblast Growth Factor Receptor, Metastasis, Dna Polymorphism						
16. SECURITY CLASSIFICATION OF:			17. LIMITATION OF ABSTRACT UU	18. NUMBER OF PAGES 52	19a. NAME OF RESPONSIBLE PERSON USAMRMC	
a. REPORT U	b. ABSTRACT U	c. THIS PAGE U			19b. TELEPHONE NUMBER (include area code)	

Table of Contents

Introduction.....	4
Body.....	4-12
Key Research Accomplishments.....	12
Reportable Outcomes.....	12
Conclusions.....	13
References.....	13
Appendices.....	14-52

INTRODUCTION

Fibroblast growth factors (FGFs) can control a multitude of cellular processes including proliferation, differentiation, survival, motility and angiogenesis. FGF2, FGF6, FGF8 and FGF17 are all expressed at increased levels in human prostate cancer and bind to FGF receptor-4 (FGFR-4) with high affinity. However, the role of FGFR-4 in human prostate cancer has not been systematically examined to date. Studies have shown that a germline polymorphism of the FGFR-4 gene resulting in expression of arginine at codon 388 (Arg^{388}) is associated with aggressive disease in patients with breast and colon cancers and sarcomas. We have found that homozygosity for the FGFR-4 Arg^{388} allele is strongly associated with the occurrence of prostate cancer in white men and the presence of the FGFR-4 Arg^{388} allele is also correlated with the occurrence of pelvic lymph node metastasis and PSA recurrence in men undergoing radical prostatectomy (1). Pooled cell lines expressing predominantly the FGFR-4 Arg^{388} or Gly^{388} allele were established by stable transfection in immortalized prostatic epithelial cells. Expression of FGFR-4 Arg^{388} resulted in increased cell motility and invasion through Matrigel when compared to cells expressing the FGFR-4 Gly^{388} allele. We hypothesize that FGFR-4, and in particular the FGFR-4 Arg^{388} variant, plays an important role in prostate cancer progression and metastasis based on correlative studies in humans. We propose to test this hypothesis in autochthonous and orthotopic mouse models of cancer. Furthermore, we hypothesize that these effects occur through specific changes in gene expression so we will carry out studies to identify changes in gene expression due to the presence of the FGFR-4 Arg^{388} allele that lead to the metastatic phenotype. Finally, we hypothesize that other cellular proteins may modulate FGFR-4 activity and may promote its transforming activities.

BODY

As outlined in our Statement of Work, we will seek to accomplish nine tasks in our three years of funding. We have accomplished or made substantial progress on all of these tasks.

Task 1: Establish and characterize pathology in transgenic mice with strong prostate specific expression of FGFR-4 Arg^{388} and Gly^{388} variants (Months 1-18)

We have established FGFR-4 transgenic mice by injection of FGFR-4 Arg^{388} and Gly^{388} cDNAs under the control of the strong prostate specific ARR2Pb promoter into mouse blastocysts. We have performed quantitative RT-PCR on RNAs extracted from the prostates of these mice. As can be seen in Figure 1, expression of FGFR-4 is approximately 100-fold higher in the transgenic mice (note that graph is log scale).

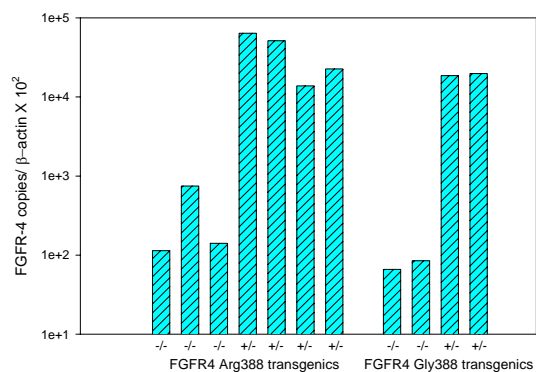


Figure 1. Expression of FGFR-4 in transgenic mice.

Expression of FGFR-4 was determined by quantitative RT-PCR in prostates from transgenic mice expressing FGFR-4 under the control of the prostate specific ARR2-Pb promoter. Note log scale.

After establishment of transgenic lines, we sacrificed mice at 2 month intervals and performed full necropsies to evaluate for

any pathology, in particular, prostatic intraepithelial neoplasia or adenocarcinoma of the prostate. Analysis reveals focal hyperplastic and dysplastic lesions in the ventral and dorsolateral prostate of transgenic mice but no invasive carcinoma has been identified to date. As expected, no pathology has been seen in other organs, since the ARR2Pb promoter is prostate specific.

Task 2: Cross FGFR-4 transgenics with TRAMP and Pb-myc mice and evaluate tumor progression (Months 12-36)

We have initiated the crosses of our FGFR-4 transgenic mice and the TRAMP or Pb-myc mice. We have currently bred more than 110 mice of the appropriate genotypes, and approximately 40% of these mice have been euthanized to date. While the exact time to euthanasia cannot be predicted in a survival study, these studies should be completed within 6 months and will be funded by available unrestricted funds. Interim analysis reveals that FGFR-4 Gly³⁸⁸ X TRAMP mice do not have any difference in survival from TRAMP littermate controls. On the other hand, FGFR-4 Arg³⁸⁸ X TRAMP mice have a shorter survival (5.2 Vs 7.0 months, P=0.07) on the interim analysis. Both of these results may change in the final analysis. Only one mouse in the Pb-myc X FGFR-4 cohort has been euthanized; this was a Pb-myc X FGFR-4 Arg³⁸⁸ transgenic that died at 7 months with extensive metastasis. This finding, while isolated, supports our hypothesis that the FGFR-4 Arg³⁸⁸ enhances metastasis. Our current plans are to complete these studies and report our results as a publication in 2008.

Task 3: Collect tumors and establish cell lines from WT TRAMP and bitransgenic mice and evaluate effect of FGFR-4 Arg³⁸⁸ and Gly³⁸⁸ on proliferation, apoptosis and motility (Months 12-36)

Task 3 is underway (see Task 2, above).

Task 4: Establishment and characterization of LNCaP and PC-3 cell lines with markedly decreased FGFR-4 expression by RNAi (Months 1-12)

We have constructed a lentivirus vector containing a SiRNA encoding sequence for FGFR-4. PC3 and LNCaP prostate cancer cells have been infected and selection performed. By quantitative RT-PCR these cell lines have 60% and 80% decreases in FGFR-4 mRNA, respectively (Fig 2). By Western blot there is a marked decrease in FGFR-4 protein in the siRNA expressing PC3 cells (Fig 3). No significant affect on cell proliferation of FGFR-4 siRNA expression was seen (data not shown), consistent with our earlier observations in PNT1a cells overexpressing FGFR-4 variants.

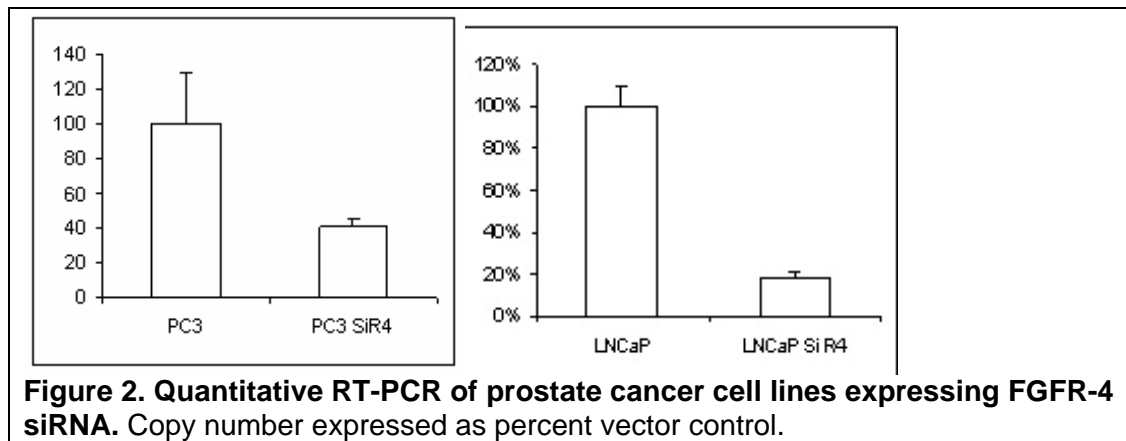


Figure 3. Western blot with anti-FGFR-4 antibody.



PC3: controls infected with empty virus; PC3 siRNA: PC3 infected with siRNA containing virus. 293 cells were transiently transfected with FGFR-4 Arg³⁸⁸ or Gly³⁸⁸ or empty vector and used for Western blot to demonstrate antibody specificity.

Task 5: Determination of the effect of decreased FGFR-4 expression in an orthotopic injection model of prostate cancer metastasis (Months 12-24)

We have carried out experiments with the PC3 SiR4 cells and PC3 control cells using an orthotopic injection model. In this model, 1X10⁶ PCa cells are injected directly into the prostate of nude mice. The cancer cells grow initially in a native prostatic environment and metastasize to pelvic and abdominal lymph nodes. We sacrificed mice 7 weeks after injection and harvested and weighed the genitourinary tract from all mice and submitted abdominal and pelvic lymph nodes for histopathological analysis. A total of 23 pathologically confirmed primary tumors were obtained in control mice and 19 in FGFR-4 ShRNA PC3 cells. Mean tumor size was significantly smaller in the tumors from the PC3 SiRNA cells compared to control (0.419 g +/- 0.136 Si Vs 0.614 +/- 0.218 control; p=0.023, t-test). More importantly, there was a significant decrease in the fraction of mice with pathologically confirmed lymph node metastasis in mice injected with the PC3 FGFR-4 ShRNA expressing cells (6 of 16 Si Vs 16 of 23 control, p=0.029, Fisher exact test). Thus, in PC3 cells decreased expression of FGFR-4 mRNA is associated with impaired progression both at the primary and local sites. It should be noted that PC3 cells are homozygous for the Arg³⁸⁸ allele, so that this effect is mediated by downregulation of this variant. It is interesting to note that the FGFR-4 Arg³⁸⁸ variant did not increase proliferation in PNTA cells and knockdown in PC3 cells did not affect proliferation, but growth at the primary site is increased. It is not clear whether this indicates that invasion enhances proliferation at primary sites, or perhaps in the native prostatic microenvironment, signals are present which promote proliferation in cells with the FGFR-4 Arg³⁸⁸ variant that are not present *in vitro*.

Similar experiments are underway with LNCaP cells. Initial analysis reveals that the primary tumors in the primary tumors in mice injected with the LNCaP SiR4 cells are significantly smaller than mice injected with control LNCaP cells (0.68 Vs 0.91 g, p=0.04, t-test). Histopathological analysis of lymph nodes is underway.

Overall, these experiments strongly support our hypothesis that FGFR-4 promotes tumor progression *in vivo*.

Task 6. Analysis of tumors from orthotopic injection model (Months 24-36)

This task is currently underway. Our current plan is complete this analysis this fall with publication of results in 2008.

Task 7: Evaluation of expression of candidate proteins mediating the biological effects of FGFR-4 Arg³⁸⁸ and correlation with FGFR-4 genotype in white patients with prostate cancer (Months 1-18)

We have evaluated expression of two candidate proteins uPAR and PAI-1 by ELISA in extracts of prostate cancers from 40 white men with prostate cancer and correlated the protein levels with FGFR-4 genotype. Of note, 7 of 40 men (17.5%) were homozygous for the FGFR-4 Arg³⁸⁸ allele. All reports to date indicate that the rate of homozygosity for the FGFR-4 Arg³⁸⁸ allele is 5-6% in the white population. Thus this is a confirmation of

our original observation that homozygosity of the FGFR-4 Arg³⁸⁸ allele is increased in white men with prostate cancer. The ELISAs did not reveal any statistically significant correlation with FGFR-4 genotype with uPAR and PAI-1 content. This may reflect the complex regulation of these factors by many genes, with FGFR-4 being only one factor of many which can control the expression of these genes.

Task 8: Identification of additional candidate genes mediating the biological effects of FGFR-4 Arg³⁸⁸ using targeted microarrays (Months 18-24)

We have identified a potential candidate gene that may mediate some of the biological effects of the FGFR-4 Arg³⁸⁸ polymorphic variant by analysis of expression microarrays. The Ehm2 gene is a member of the NF2/ERM/4.1 superfamily. Members of this superfamily all contain a FERM domain and are involved in membrane-cytoskeletal interactions. There is a strong correlation between Ehm2 gene expression and the metastatic potential of K-1735 and B16 melanoma cells (2). It is proposed that alterations of the expression level of Ehm2 are likely to be linked to one or more steps of cancer metastasis through regulation of interaction between cell surface transmembrane

proteins and cytoskeletal proteins. Ehm2 is expressed at higher levels in PNT1A cells expressing FGFR-4 Arg³⁸⁸ when compared to cells expressing equivalent amounts of FGFR-4 Gly³⁸⁸ (Figure 4A) and knockdown of FGFR-4 decreases Ehm2 (Fig 4B).

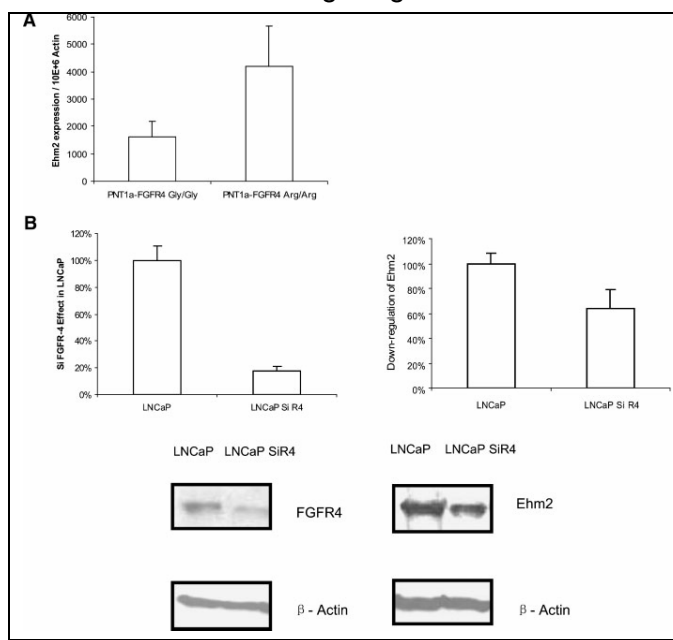


Figure 4. FGFR-4 increases Ehm2 expression. **A.** Expression was quantitated using real-time RT-PCR of RNAs from PNT1a cells overexpressing the Arg³⁸⁸ or Gly³⁸⁸ variant. Data was normalized using β-actin transcript levels. **B.** SiRNA against FGFR-4 decreases FGFR4 and Ehm2 expression in LNCaP cells at the RNA and protein level

To analyze expression of Ehm2 at the protein level *in vivo* we performed immunohistochemical analysis of Ehm2 expression using a prostate cancer tissue microarray containing 32 matched normal and prostate cancer tissues. Staining was predominantly seen in benign and malignant epithelial cells (Figure 5) with some staining of smooth muscle. Stained slides were digitized and scored both for extent of staining (scale of 0-3) and intensity of staining (scale of 0-3). An average staining index was calculated from the extent of staining score for the three cores multiplied by the staining intensity score so that the staining index ranged from 0 (no staining) to 9 (extensive, strong staining). Normal prostate epithelium showed a staining index of 6.3 +/- 0.38 (mean +/- SEM) while the cancer tissues had a staining index 7.4 +/- 0.29. This difference was statistically significant ($p < 0.05$, Mann Whitney).

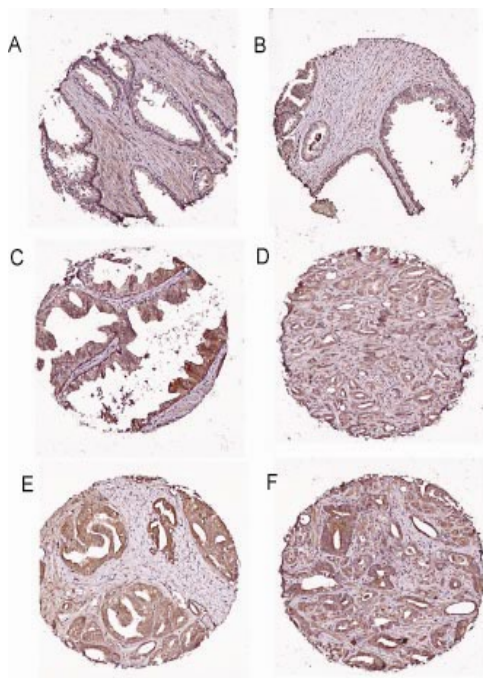


Figure 5. Expression of Ehm2 in normal prostate and prostate cancer.

Immunohistochemistry with anti-Ehm2 antibody was performed using a tissue microarray of normal and prostate cancer tissues. A. Normal prostate with weak staining of epithelium. B. Normal prostate with moderate epithelial staining. C. High grade prostatic intraepithelial neoplasia with strong staining. D. Prostate cancer with moderate staining. E, F. Prostate cancers with strong staining.

Overall, 27% of normal tissues showed low staining (index<6.0) while only 10% of cancers had low staining. In contrast, 40% of cancers showed maximal staining intensity (index =9) Vs 8% of normal epithelium. Of note was the finding that none of the cases with low Ehm2 staining (staining index<6.0) had a PSA recurrence, while all cases with recurrence had moderate to strong Ehm2 staining (staining index 6-9). This difference is statistically significant ($p=0.03$, Fisher exact test).

Ehm2 may regulate cytoskeleton interactions with transmembrane proteins and thus affect cancer cell adhesion. To evaluate the impact of Ehm2 on adhesion, we carried out two series of complementary experiments. PNT1a cells, which express low levels of Ehm2, were transiently transfected with an expression vectors containing the Ehm2 cDNA. Two cDNAs were used: a full-length form and a 5' truncated variant that would give rise to a smaller protein that is the main protein seen in prostate epithelial cells ((3); see attached manuscript for details). The results of these experiments are shown in Figure 6A. Ehm2 expression was increased 8 or 17-fold in the transfected cells and this was associated with a 30% decrease in adhesion to collagen IV. We then decreased Ehm2 mRNA in the LAPC4 cell line, which showed the second strongest Ehm2 expression among tested prostate cell lines, using siRNA. As shown in Fig 6B, 24h after siRNA transfection, there was an approximately 50% decrease in Ehm2 transcript level, while adhesion to collagen IV increased about 20% compared to control cells. These results indicate that Ehm2 expression is associated with decreased adhesion to collagen IV by prostatic epithelial cells. Collagen IV adhesion has been previously shown to be inversely correlated with metastatic behavior in breast cancer (4). All experiments were repeated 3 times and ranges are shown.

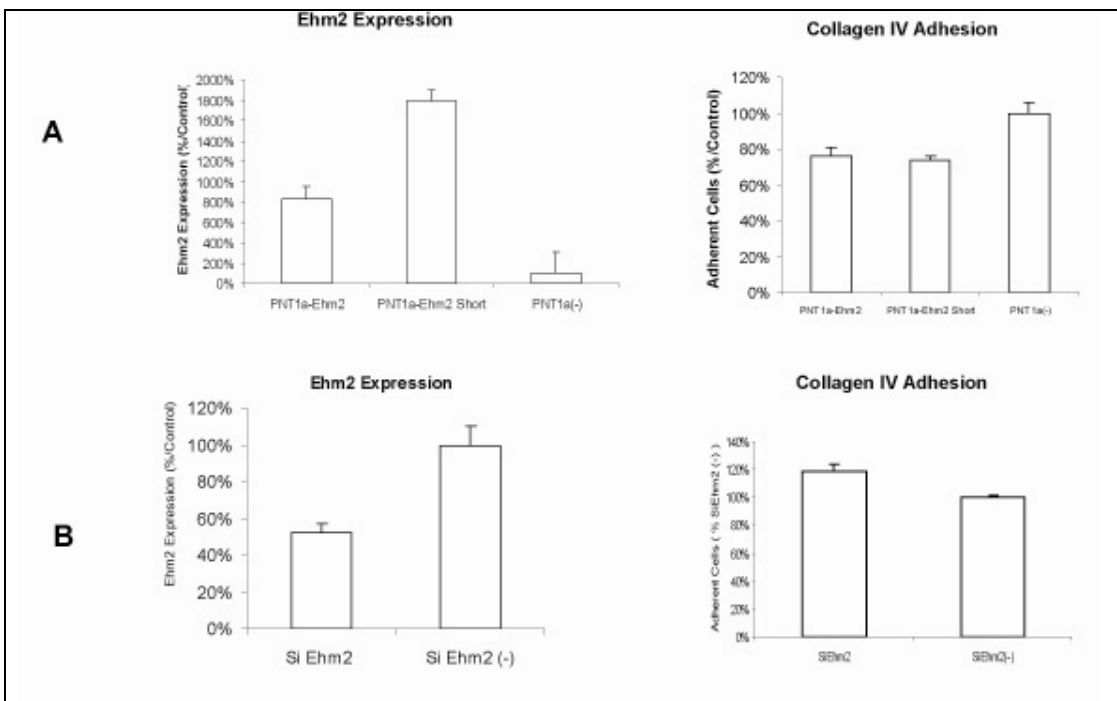


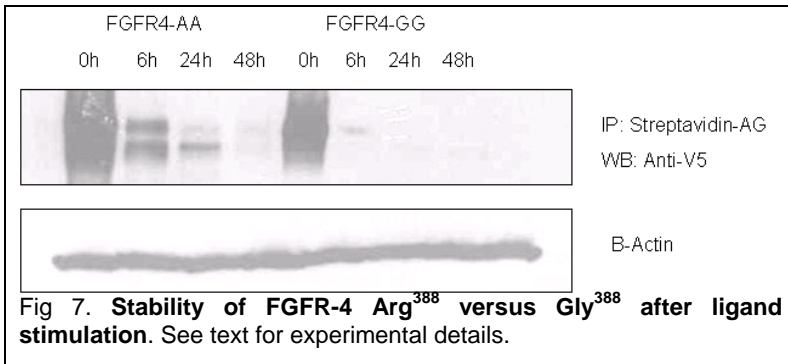
Figure 6. Ehm2 expression results in decreased collagen IV adhesion

A. PNT1A cells were transiently transfected with full length or 5' truncated Ehm2 cDNA cloned into the pCMV-Tag2b expression vector or empty vector. Expression of Ehm2 in transfectants by quantitative RT-PCR (left). Collagen IV adhesion of Ehm2 and control PNT1A tranfected cells (right). One of 3 experiments with similar results is shown.
B. LAPC4 prostate cancer cells were transiently transfected with Ehm2 or control siRNA. Expression of Ehm2 in transfectants by quantitative RT-PCR (left) Collagen IV adhesion of Ehm2 siRNA and control siRNA transfected LAPC4 cells (right). Range of triplicate determinations is shown.

In summary, we have identified Ehm2 as a gene which can promote metastasis that is upregulated by expression of the FGFR-4 Arg³⁸⁸ allele. A manuscript describing these findings (including additional data not presented in this report) was recently published in *Prostate* (3) and a copy is appended.

Task 9: Evaluation of expression of candidate proteins mediating the biological effects of FGFR-4 Arg³⁸⁸ and correlation with FGFR-4 genotype in white patients with prostate cancer (Months 24-36)

We have also sought additional proteins that may mediate the biological effects of FGFR-4 using a hypothesis-based approach. Given that the expression of the FGFR-4 Arg³⁸⁸ variant is associated with aggressive disease, an important question remains: what is the molecular basis for the difference between the two FGFR-4 variants? Achondroplasia (dwarfism) is caused by a similar mutation in FGFR-3 (Gly³⁸⁰ to Arg³⁸⁰). Increased FGFR-3 signaling due to this mutation inhibits proliferation in chondrocytes. Elegant studies have shown that this mutation leads to decreased receptor turnover due to increased receptor recycling and decreased targeting of receptors to lysosomes. We therefore sought to determine if a similar phenomenon occurs with the FGFR-4 Arg³⁸⁸ variant. To assess receptor stability, we biotinylated cell surface receptors and



Western blots with anti-V5 antibody recognizing a V-5 tag on the transfected FGFR-4 variants. As can be seen in Fig 2, the FGFR-4 Arg³⁸⁸ variant is much more stable than the Gly³⁸⁸ variant. We have repeated this experiment multiple times with essentially identical results. The molecular basis for the increased receptor stabilization is unclear. It could be due to decreased rate of internalization or degradation or increased recycling from the endosome compartment or some combination of these. We have also shown that this receptor stabilization is associated with sustained receptor activation (data not shown).

Based on these studies, we have begun to investigate other proteins that can potentially modulate stability or turnover of FGFR-4. One such protein is HIP1 (Huntington interacting protein 1). HIP1 interacts with Huntington, the gene mutated in Huntington's chorea. HIP1 can interact with clathrin as well alpha-adaptin, which is part of the AP-2 late endocytic complex. Work by the Ross group has been shown that HIP1 can stabilize EGF receptors. The primary site of such stabilization appears to be via stabilization in early endosomes. Over-expression of HIP1 leads to transformation of NIH3T3 cells. Of note, the Ross group has shown by IHC that HIP1 expression is increased in prostate cancer and that absence of HIP1 is associated with favorable

outcome. Using quantitative RT-PCR (Fig 8) we have found that HIP1 mRNA is significantly increased in prostate cancer ($p=0.018$, Mann-Whitney Test) and is higher in cancers with biochemical recurrence following radical prostatectomy versus those with no recurrence ($p=0.05$). Thus, HIP1 may play an important role in promoting prostate cancer aggressiveness. To determine the biochemical and biological effects of HIP1 on FGF signalling and FGF receptor-4 we established cell lines from PNT1A and LNCaP cell lines expressing HIP1 under a constitutive promoter.

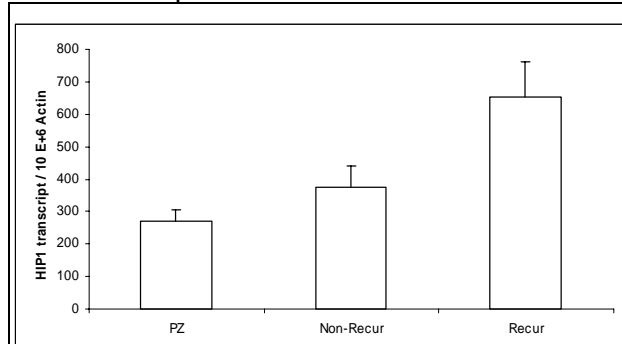


Fig 8. Expression of HIP1 in prostate cancer. Q-PCR of mRNAs from normal prostate (PZ), BPH, and PCa with no PSA recurrence at 5 years (non-recur), or PSA recurrence (less than 1 year; early-recur) following radical prostatectomy. Normalized to β -actin

promoter. As can be seen in Fig 9, for both types of cells, expression of HIP1 in a clone was associated with markedly increased FGFR-4 expression. Quantitative RT-PCR to determine FGFR-4 receptor expression levels revealed no increase, and in most cases, slight decreases in FGFR-4 mRNA levels. Thus HIP1 increases FGFR-4 protein via a post-transcriptional mechanism. Using transient transfection in 293T cells and labeling of surface receptors with biotin (as in Fig 7), we have found that HIP1 appears to specifically increase stability of the FGFR-4 Gly³⁸⁸ variant (Fig 10). Note that both

PNT1A and LNCaP cells have an Arg³⁸⁸/Gly³⁸⁸ genotype so that the effects seen in 293T cells are consistent with the results seen in the stable cell lines from these cells (Fig 9). Reciprocal IP-Western blot studies have shown a direct interaction of both forms of FGFR-4 with HIP1 and

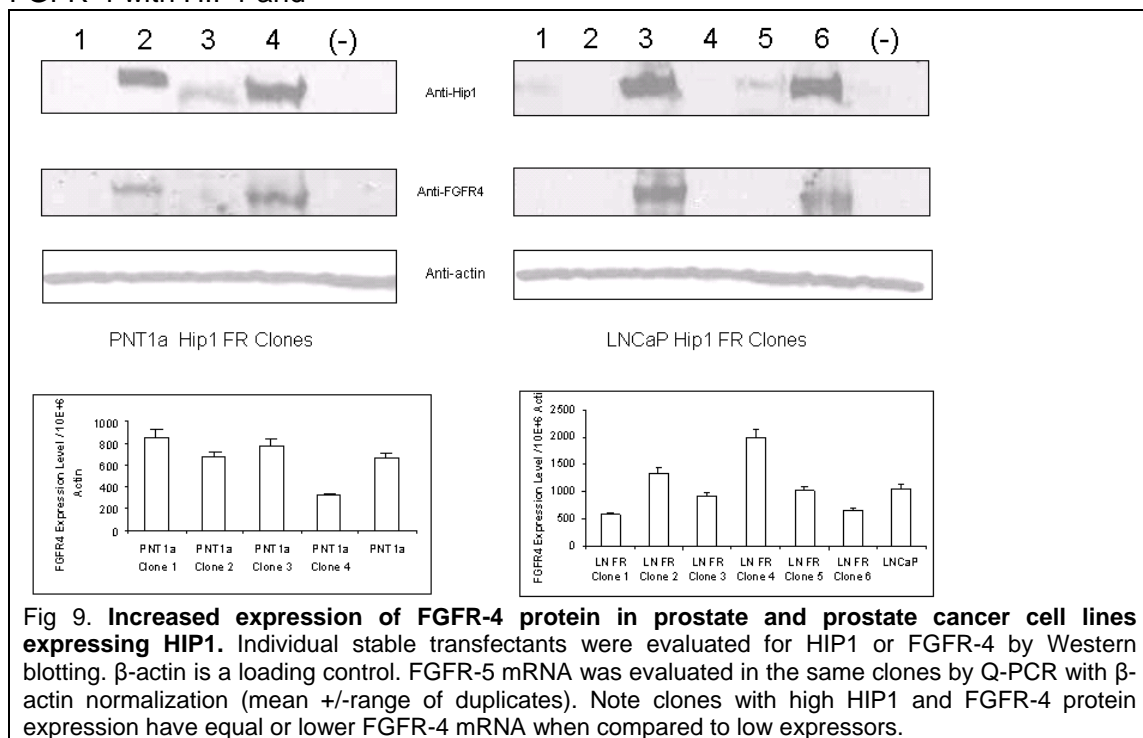


Fig 9. Increased expression of FGFR-4 protein in prostate and prostate cancer cell lines expressing HIP1. Individual stable transfectants were evaluated for HIP1 or FGFR-4 by Western blotting. β -actin is a loading control. FGFR-5 mRNA was evaluated in the same clones by Q-PCR with β -actin normalization (mean +/- range of duplicates). Note clones with high HIP1 and FGFR-4 protein expression have equal or lower FGFR-4 mRNA when compared to low expressors.

studies with deletion constructs have shown that the region between amino acids 601-798 of HIP1 are required for this interaction (data not shown). We next examined the biological effects of HIP1 expression. In both PNT1A and DU145 cells, expression of full length HIP1 (FR) increases proliferation in media containing FGF2 and insulin as the only growth factors (Fig 11). This effect was not seen with a truncated receptor (F2R). (Note that DU145 are homozygous for the Gly³⁸⁸

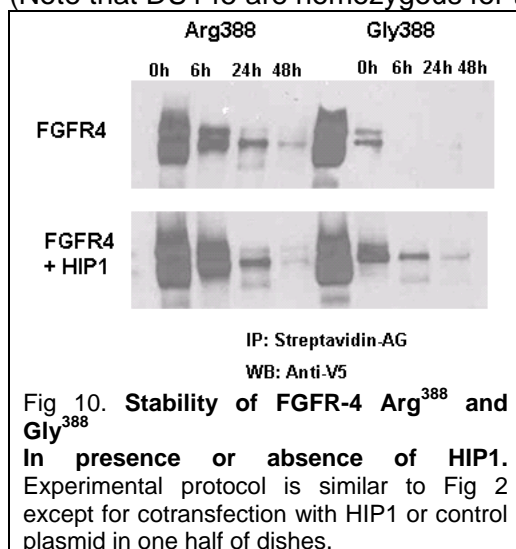


Fig 10. Stability of FGFR-4 Arg³⁸⁸ and Gly³⁸⁸ in presence or absence of HIP1. Experimental protocol is similar to Fig 2 except for cotransfection with HIP1 or control plasmid in one half of dishes.

allele.) Similar increases in proliferation were seen in serum-containing medium that were abolished by downregulation of FGFR-4 with siRNA (data not shown). These results imply that, even in complex media containing a variety of growth factors, FGFR-4 is a major effector of HIP1-mediated proliferation. PNT1A cells are immortalized and not fully transformed and do not form colonies in soft agar. Expression of HIP1 leads to colony formation in soft agar (Fig 12). Downregulation of FGFR-4 by 50% with siRNA partially abolishes this phenotype, (Fr Vs FiSiR4, $p=0.03$), again implying that FGFR-4 plays a role in mediating HIP1 effects even in serum-containing medium. A manuscript reporting the data presented above has been submitted to

Cancer Research and a copy is attached.

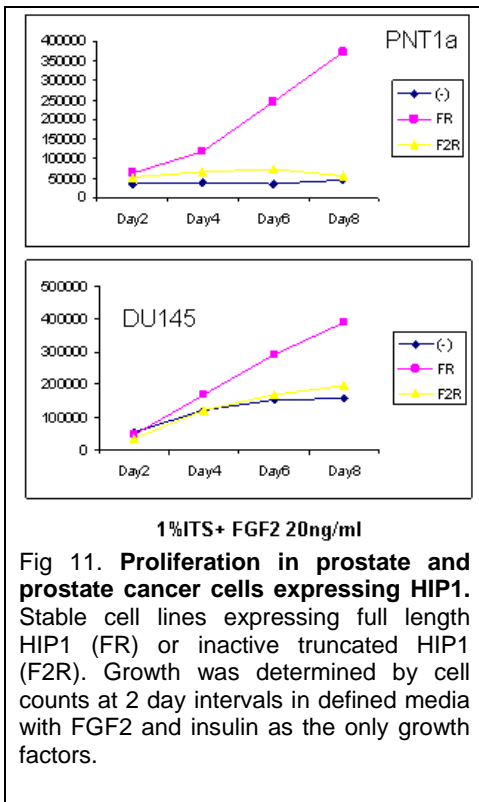


Fig 11. Proliferation in prostate and prostate cancer cells expressing HIP1. Stable cell lines expressing full length HIP1 (FR) or inactive truncated HIP1 (F2R). Growth was determined by cell counts at 2 day intervals in defined media with FGF2 and insulin as the only growth factors.

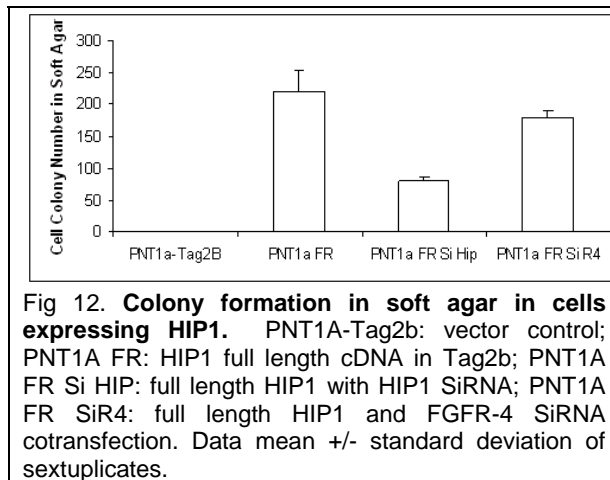


Fig 12. Colony formation in soft agar in cells expressing HIP1. PNT1A-Tag2b: vector control; PNT1A FR: HIP1 full length cDNA in Tag2b; PNT1A FR Si HIP: full length HIP1 with HIP1 SiRNA; PNT1A FR SiR4: full length HIP1 and FGFR-4 SiRNA cotransfection. Data mean +/- standard deviation of sextuplicates.

In summary, our published and unpublished data indicates that the presence of the FGFR-4 Arg³⁸⁸ variant is associated with both PCa initiation and progression in humans and in a mouse model. This is correlated with increased invasion and motility *in vitro* and expression of genes, such as uPAR and Ehm2, which are associated with metastasis in other systems. Our current data indicates that the FGFR-4 Arg³⁸⁸

variant has increased receptor stability and/or decreased degradation, which may well underlie its ability to promote prostate cancer initiation and progression. FGFR-4 associates with HIP1 and the Gly³⁸⁸ variant is significantly stabilized by this interaction and results in phenotypes associated with cancer, including increased proliferation in low growth factor conditions and colony formation in soft agar. An important next step will be a comprehensive analysis of FGFR-4 genotype, FGFR-4 protein expression, HIP1 expression and patient outcome in a large series of patients.

KEY RESEARCH ACCOMPLISHMENTS

- * Establishment and initial characterization of FGFR-4 Arg³⁸⁸ and Gly³⁸⁸ transgenic mice.
- * Mating of FGFR-4 transgenic mice to TRAMP and Pb myc transgenic mice.
- * Construction of FGFR-4 siRNA lentivirus and establishment of PC3 and LNCaP FGFR-4 siRNA cell lines
- * Carried out orthotopic injection experiments establishing that FGFR-4 promotes prostate cancer progression *in vivo*.
- * Identification of Ehm2 as an FGFR-4 Arg³⁸⁸ regulated gene and characterization of its role in prostate cancer.
- * Identification of HIP1 as an important modulator of FGFR-4 activity in prostate cancer.

REPORTABLE OUTCOMES

- * Establishment of FGFR-4 Arg³⁸⁸ and Gly³⁸⁸ transgenic mouse lines
- * Establishment of PC3 and LNCaP FGFR-4 SiRNA cell lines
- * Publication of manuscript describing role of Ehm2 in prostate cancer ((3) see attached)
- * Manuscript submitted to Cancer Research describing interaction of HIP1 with FGFR-4

CONCLUSION

Our published data indicates that FGFR-4 plays an important role in prostate cancer initiation and progression. We have now proven that FGFR-4 plays an important role in prostate cancer progression *in vivo*. We have established that Ehm2 plays an important role in this process. Furthermore, HIP1 plays an important role in modulating FGFR-4 Gly388 activity and is associated with more aggressive prostate cancer.

REFERENCES

- 1) Wang, J., Stockton, D. W., and Ittmann, M. (2004) The fibroblast growth factor receptor-4 Arg388 allele is associated with prostate cancer initiation and progression. *Clin Cancer Res* 10, 6169-6178
- 2) Shimizu, K., Nagamachi, Y., Tani, M., Kimura, K., Shiroishi, T., Wakana, S., and Yokota, J. (2000) Molecular cloning of a novel NF2/ERM/4.1 superfamily gene, ehm2, that is expressed in high-metastatic K1735 murine melanoma cells. *Genomics* 65, 113-120
- 3) Wang, J., Cai, Y., Penland, R., Chauhan, S., Miesfeld, R.L., and Ittmann, M. (2006) Increased expression of the metastasis-associated gene Ehm2 in prostate cancer. *Prostate* 66:1641-1645
- 4) Gui, G., Puddefoot, J., Vinson, J., Wells, C., and Carpenter, R. (1997) Altered cell-matrix contact: a prerequisite for breast cancer metastasis? *Br J Cancer* 75, 623-633

Increased Expression of the Metastasis-Associated Gene Ehm2 in Prostate Cancer

Jianghua Wang,¹ Yi Cai,¹ Rebecca Penland,¹ Sanjay Chauhan,²
Roger L. Miesfeld,² and Michael Ittmann^{1*}

¹Department of Pathology of Baylor College of Medicine and Michael E. DeBakey Department of Veterans Affairs Medical Center, Houston, Texas

²Department of Biochemistry and Molecular Biophysics, University of Arizona, Tucson, Arizona

BACKGROUND. Alterations of fibroblast growth factors and their receptors contribute to prostate cancer progression by enhancing cell survival, motility, and proliferation. The expression of the FGFR-4 Arg³⁸⁸ variant is correlated with the occurrence of pelvic lymph node metastasis and biochemical (PSA) recurrence in men undergoing radical prostatectomy. Ehm2 is an androgen-regulated gene that has been associated with metastasis in other systems, so we sought to determine if it is expressed in prostate cancer and if the FGFR-4 Arg³⁸⁸ variant can increase its expression.

METHODS. Expression of Ehm2 was examined by quantitative RT-PCR and Western blotting in prostate cell lines and by quantitative RT-PCR, *in situ* hybridization, and immunohistochemistry in prostate tissues. The effect of Ehm2 expression on collagen IV adhesion was tested by transient overexpression and RNA interference.

RESULTS. Ehm2 expression is upregulated in prostate cancer cell lines and prostate cancer tissues. Expression of the FGFR-4 Arg³⁸⁸ variant results in increased expression of Ehm2. Increased expression of Ehm2 leads to decreased adhesion to collagen IV, which has been associated with metastasis in cancers. Analysis of tissue microarrays revealed that increased Ehm2 expression is associated with biochemical recurrence after radical prostatectomy, which is indicative of more aggressive disease.

CONCLUSIONS. Ehm2 is overexpressed in prostate cancer and may enhance disease progression and metastasis. *Prostate* 66: 1641–1652, 2006. © 2006 Wiley-Liss, Inc.

KEY WORDS: Ehm2; prostate cancer; recurrence; cell adhesion; metastasis

INTRODUCTION

Prostate cancer is the most common visceral malignancy in US men, with approximately 230,000 new cases and 29,000 deaths in 2004 [1]. Prostate cancer deaths are a result of metastatic disease and treatment of such metastatic disease is one of the major therapeutic challenges in prostate cancer treatment. Many studies have been focused on identification of the biological mechanisms of metastasis in prostate cancer and significant insights into the basis of prostate cancer metastasis have emerged from these studies [2–7]. Malignant tumors are heterogeneous with regard to metastatic potential, and prostate cancer cells with high- and low-metastatic potential vary in their biological properties, such as proliferation,

adhesiveness, invasiveness, and motility. This variation is a result of both germline variation between

Grant sponsor: Department of Defense Prostate Cancer Research Program; Grant number: W81XWH-04-1-0843; Grant sponsor: Department of Veterans Affairs Merit Review program; Grant sponsor: National Cancer Institute to the Baylor prostate cancer SPORE program; Grant number: P50CA058204; Grant sponsor: Jack Findlay Doyle II Charitable Fund.

*Correspondence to: Michael Ittmann, MD, PhD, Michael E. DeBakey VAMC, 2002 Holcombe Blvd, Houston, TX 77030.

E-mail: mittmann@bcm.tmc.edu

Received 3 November 2005; Accepted 11 April 2006

DOI 10.1002/pros.20474

Published online 22 August 2006 in Wiley InterScience (www.interscience.wiley.com).

individuals [7] and somatic alterations of genes and gene expression in cancer cells [2–6]. Despite recent advances, our understanding of the process by which prostate cancer cells metastasize to distant sites remains imperfect.

Fibroblast growth factors (FGFs) can control a multitude of cellular processes including proliferation, differentiation, survival, motility, and angiogenesis. FGF2, FGF6, FGF8, and FGF17 are all expressed at increased levels in human prostate cancer and bind to FGF receptor-4 (FGFR-4) with high affinity [8]. Studies have shown that a germline polymorphism of the FGFR-4 gene resulting in expression of arginine at codon 388 (Arg³⁸⁸) is associated with aggressive disease in patients with breast and colon cancer [9] as well as other malignancies [7,10,11], although in some patient populations, these associations have not been present for breast and colon cancer [12,13]. We have found that the presence of the FGFR-4 Arg³⁸⁸ allele is correlated with the occurrence of pelvic lymph node metastasis and biochemical (PSA) recurrence in men undergoing radical prostatectomy [7]. Pooled cell lines expressing predominantly the FGFR-4 Arg³⁸⁸ or Gly³⁸⁸ allele were established by stable transfection in immortalized prostatic epithelial cells (PNT1a cells), and expression of FGFR-4 Arg³⁸⁸ variant resulted in increased cell motility and invasion through Matrigel when compared to cells expressing the FGFR-4 Gly³⁸⁸ variant. Further analysis of PNT1a cells overexpressing the FGFR-4 Arg³⁸⁸ variant revealed that increased expression of the urokinase plasminogen activator receptor may be involved in the increased metastasis seen in cells bearing the Arg³⁸⁸ allele. It is likely that other genes may also be involved in increasing the metastatic potential of FGFR-4 Arg³⁸⁸ expressing prostate cancer cells.

One gene that has been linked to metastasis is *Ehm2*. The *Ehm2* gene is a member of the NF2/ERM/4.1 superfamily [14]. Members of this superfamily all contain a FERM domain and are involved in membrane–cytoskeletal interactions. Hashimoto et al. [15] demonstrated a good correlation between *Ehm2* gene expression and the metastatic potential of mouse K-1735 and B16 melanoma cells. They proposed that alterations of the expression level of *Ehm2* are likely to be linked to one or more steps of cancer metastasis through regulation of interaction between cell surface transmembrane proteins and cytoskeletal proteins [15]. Human *Ehm2* was recently characterized in a human fibrosarcoma cell line model of steroid-regulated cytoskeletal reorganization and shown to be androgen-regulated [16]. Moreover, a related FERM domain protein, ezrin, was reported to be androgen-regulated in the rat prostate [17] and also overexpressed in metastatic rhabdomyosarcomas [18]. Since FGFR-4 is a

transmembrane protein that can interact with multiple other cell surface proteins, we sought to determine if expression of the FERM domain protein *Ehm2* is increased in prostate cancer cells containing the FGFR-4 Arg³⁸⁸ variant.

We report here that expression of the FGFR-4 Arg³⁸⁸ variant results in increased expression of *Ehm2* in prostate epithelial cells. To further characterize the function of *Ehm2* in prostate cancer, we carried out a systematic study of *Ehm2* expression by quantitative real-time PCR and immunohistochemistry. *Ehm2* expression is upregulated in prostate cancer cell lines and prostate cancer tissues. Increased expression of *Ehm2* leads to decreased adhesion to collagen IV, which has been associated with metastasis in cancers. Analysis of tissue microarrays revealed increased *Ehm2* expression that is associated with biochemical recurrence following radical prostatectomy, which is indicative of more aggressive disease. Thus, *Ehm2* is overexpressed in prostate cancer and may enhance disease progression and metastasis.

MATERIALS AND METHODS

Tissue Culture

PNT1a, an immortalized normal prostatic epithelial cell line, was obtained from the European Collection of Animal Cell Cultures (Porton Down, United Kingdom). PC3 and LNCaP cell lines were obtained from the American Type Culture Collection. All cell lines were cultured in RPMI-1640 (Invitrogen, Carlsbad, CA) supplemented with 10% fetal bovine serum. The LAPC4 cell line, which was established from the LAPC4 human prostate cancer xenograft [19], was kindly provided by Dr. Charles Sawyers (University of California, LA). It was maintained in 1× Iscoves (Invitrogen) with 10% FBS, 1% PenStrep (Invitrogen), 1% L-Glutamine (Invitrogen), and supplemented with 10 nM R1881 (Perkin Elmer Life Sciences, Boston, MA).

Human Prostate Tissue Samples

All samples of human prostate tissues were obtained with informed consent and maintained by the Baylor Specialized Program of Research Excellence (SPORE) in the prostate cancer tissue bank. Fresh frozen tissue punches of normal and tumor tissue were obtained at the time of radical prostatectomy as described previously [20]. The pathological status was confirmed before processing, and the tumor samples had a tumor cell percentage of 70–100%. Normal peripheral zone and hyperplastic transition zone samples were free of tumor.

RNA Extraction, cDNA Synthesis, and Quantitative Real-Time PCR

RNA was extracted as described previously [21] from 86 tissue samples collected from radical prostatectomies by Baylor Prostate SPORE Tissue Core. There were 19 normal samples (peripheral zone tissue), 20 early recurrence cancers (PSA recurrence in less than 1 year), 19 late recurrence cancers (PSA recurrence after 1–5 years), 20 non-recurrent samples (no PSA recurrence in 5 years), and 8 benign prostate hyperplasia (BPH) samples. Primers for Ehm2 were located between exon 8 and 11 (Genebank number: AB032179) and were as follows: Ehm2 Forward: 5'-GCGAAGTGGCTGGAAAT GTATG-3' Reverse: 5'-GAAGAATGCGTGG TGCTAAC-3'. Control β-Actin primer has been described previously [21]. Five micrograms of each RNA sample was reversed transcribed into cDNA in a total volume of 100 μl by using iScript cDNA Synthesis kit (BioRad Laboratories, Hercules, CA) according to the manufacturer's protocol. Real-time PCR was carried out in a final reaction volume of 25 μl by using 5 μl of the template cDNA or standard control vector which contained genes of interest. The Mastermix for real-time PCR contained 2 mM MgCl₂, 0.4 μM each forward and reverse primers, and 2.5 μl of LC-FastStart DNA Master SYBR GREEN (10×; Roche, Indianapolis, IN). Real-time PCR was done by using the iCycler IQ instrument from Bio-Rad. β-Actin, Genebank Access BC004251, plasmid (ATCC#MGC-10559) was purchased from American Type Culture Collection. The Ehm2 plasmid was constructed into PCR 2.1-Topo vector from Topo TA Cloning Kit (Invitrogen). Plasmids were prepared by using the Qiagen Spin Mini-prep Kit (Qiagen, Inc., Valencia, CA). Quantification of plasmid was performed using a UV/Visible spectrophotometer. The plasmid concentration was converted into copy number, a dilution series of each plasmid from 10⁸ to 10² were used as DNA standard for real-time PCR. All real-time PCR efficiencies were controlled in the range of 100% ± 5.

Western Blotting

Total protein was extracted from cells using RIPA lysis buffer (Santa Cruz Biotechnology, Santa Cruz, CA). For Western blots, 40 μg of protein extract/lane were electrophoresed, transferred to nitrocellulose membrane (Hybond ECL; Amersham Biosciences, Piscataway, NJ), and incubated overnight with a 1:200 dilution of anti-Ehm2 F19 goat polyclonal antibody (Santa Cruz), which was raised against a peptide mapping an internal region of EHM2 of human origin, a 1:1,000 dilution of anti-Flag M2 monoclonal antibody (Stratagene), an anti-FGFR4 antibody (1:500; Santa

Cruz) or anti-β-actin (1:5,000, Sigma). Membranes were washed and treated with mouse anti-goat IgG (1:5,000; Santa Cruz), mouse anti-rabbit (1:10,000, Santa Cruz) or goat anti-mouse IgG secondary antibody (1:5,000, Pierce Biotechnology, Rockford, IL) conjugated to horseradish peroxidase. The antigen-antibody reaction was visualized using an enhanced chemiluminescence (ECL) assay (Amersham Biosciences) and exposed to ECL film (Amersham Biosciences).

In Situ Hybridization of Prostate Tissues

The human Ehm2 sequence was obtained by PCR using primers with EcoRI and SalI at both ends: Ehm2 Tag Forward: TAGAATTCATGCTGCGGTTCCTGC and Ehm2 Tag Reverse: GAGCGTCGAC TCAAAGTG-CAGTCAT from LNCaP cell line. The Ehm2 PCR fragment was cloned into EcoRI/SalI site of pCMV-Tag2B vector (Stratagene, La Jolla, CA), which has T3 and T7 at both ends of the insert to be used to generate sense and anti-sense RNA probes. Digoxigenin-labeled antisense and sense RNA probes were synthesized using MAXIscript in vitro RNA transcription kit (Ambion, Inc., Austin, TX) and a linearized plasmid with the Ehm2 gene fragment as templates. Tissue slides containing 12 prostate tissues were used. In situ hybridization was carried out by standard procedures. Briefly, prostate tissues were de-waxed in xylene, 3 × 10 min, hydrated, digested with 40 μg/ml proteinase K for 7 min at room temperature, fixed in 4% paraformaldehyde for 20 min. One microgram Dig-labeled probe was used for 1 ml hybridization buffer (50% formamide, 10% SSC). Hybridization was performed at 70°C overnight, after which slides were sequentially washed by Dig Wash and Block Buffer Set (Roche Diagnostics, Indianapolis, IN) following manufacturer's protocol. Anti-digoxigenin antibody (1:2,000) was used to detect the signal and NBT/BCIP was used as substrate for color development (Boehringer Mannheim, Germany).

Immunohistochemistry Using Tissue Microarray

A prostate cancer tissue array was obtained from the Baylor Prostate Cancer SPORE containing 32 cases prostate cancer from men undergoing radical prostatectomy. Each case was represented by five 0.2-mm punches of normal peripheral zone or cancer tissue. Immunohistochemistry was carried out as described previously [22]. Primary antibody incubation was carried out at 4°C overnight at a 1:300 dilution using a goat polyclonal anti-Ehm2 antibody (F21; Santa Cruz Biotechnology), which was raised against a peptide mapping near the carboxy terminus of Ehm2 of mouse origin followed by the avidin-biotin peroxidase complex procedure (Vector Laboratories, Inc.,

Burlingame, CA). Slides were digitized and staining was evaluated semi-quantitatively in normal epithelium and prostate cancer by a pathologist (M.I.). Expression in normal or neoplastic prostatic epithelium was scored according to the intensity and percentage of stained tumor and normal prostate glands as described previously. Atrophic or metaplastic glands were not scored. Weak staining was graded as 1, intermediate staining was considered as 2, and strong staining was considered 3. As for the percentage of stained glands, 1 stands for 1~33% glands with staining, 2 for 34~66%, and 3 for 67~100%, respectively. The staining index was calculated as the product of the intensity and percent score, resulting in a staining index ranging from 0 (no staining) to 9 (extensive, strong staining). The mean score of the five cores was then calculated for each case. Of the 32 cases, 27 normal and 30 cancer cases gave usable data, with some cases lost due to technical artifacts or absence of appropriate epithelium after multiple previous sections. In two cases, no clinical follow-up was available. As a negative control, a fivefold molar excess of blocking peptide incubated for 2 hr at room temperature with antibody to generate a negative control antibody. Immunohistochemistry with this pre-incubated antibody showed no staining (data not shown).

Cloning of Ehm2 cDNA and Transient Transfection

The 1,557-bp Ehm2 cDNA was generated by PCR using total RNA isolated from dihydrotestosterone-treated HT-AR1 cells [16] and a 5' primer with the sequence 5'-ATGCTGCGGTTCCCTGCGGCC GGAC-3' that also included a single FLAG epitope coding sequence and a HindIII cloning site, and a 3' primer containing the EHM2 sequence 5'-AGTCTCTCAAAGT GCAGTCAT-3' and a BamHI cloning site. The PCR reaction was performed using the GC-RICH PCR system from Roche Diagnostics following the manufacturer's recommendations. The PCR product was digested with HindIII and BamHI and cloned into the pcDNA 4/TO vector (Invitrogen) and sequenced. For expression studies, the full length Ehm2 fragment was excised with HindIII and BamH1 and cloned into the pCEP4 expression vector. A shorter Ehm2 fragment was also cloned from LNCaP cells which lacked 258 bp of 5' sequence compared to full length Ehm2 cDNA. Transient transfection of 293T cells using both Ehm2 expression vectors verified the expression of full length and short form Ehm2 proteins by Western blot using an anti-Flag M2 antibody prior to transfection of PNT1a cells. PNT1a cells were plated at 2×10^6 cells per 100-mm dish 24 hr before transfection and transfected with 20 μ l Fugene6 (Invitrogen) and 7 μ g of plasmid (pCEP4-

Ehm2, pCMV-Tag2B-Ehm2 or control vector) for 5 hr in a total volume of 4 ml of RPMI 1640 medium without serum. One milliliter of FBS was then added to each dish to achieve a final serum concentration of 20%. Cells were refed with complete medium on Day 2. After an additional 24 hr incubation, cells were used to perform collagen IV assays as described below or used for RNA extraction.

Generation of Ehm2 SiRNA and Transfection

SilencerTM siRNA Cocktail Kit (Ambion) was used to decrease the expression of Ehm2 in LAPC4 cell line. To prepare the DNA template for generating SiEhm2, amplification strategy of a single PCR with the T7 promoter appended to both PCR primers was used. Primers, which amplified a fragment of ~400 bp located at 5' end of Ehm2 sequence, were used. siEhm2F: 5'-TAATACGACTCACTATAGGGAGG AT GCTGCGGTTCCCTG-3'; siEhm2R: 5'-TAATACGACT-CACTATAGGGCAAGCT CCGCTTGAGAC-3'. To generate SiRNA, the RNA transcript from this PCR product was digested following the manufacturer's instruction protocol to yield 12–15 bp oligonucleotides, which were stored at a concentration of 20 μ M at –20°C. LAPC4 cells were treated with this Si-Ehm2 oligonucleotides mix at 200 nM using OligofectamineTM Reagent (Invitrogen). The LAPC4 cells were seeded at 3×10^5 in 6-well plates 24 hr before the transfection in Opti-MEM I Reduced Serum Medium. Four hours after initiation of transfection, growth medium containing three times the normal concentration of serum was added without removing the transfection mixture. RNA was extracted 24 hr post-transfection and Ehm2 transcript level determined by RT-PCR or cells plated for to determine collagen IV adhesion as described below.

SiFGFR-4 in LNCaP Cells

To investigate if Ehm2 expression can be modulated by reduced FGFR-4 expression, we generated a LNCaP cell line with stably reduced FGFR-4 expression using Block-iTTM Lentiviral RNAi Expression System (Invitrogen). Primers used for Lentiviral construct were: SiR4Top 5'-CA CCGCATA GGGACCTCTCGA ATATT CGAAAATATTGAGAGGTCCCTATGC-3' SiR4Bot 5'-AAAAGCATAGGGACCTCTCGAATATT TTCGA ATATTGAGAGGTCCCTATGC-3'. Lentiviral construct was generated according to manufacturer's instruction. Lentivirus which stably expresses the shRNA of FGFR-4 was produced by 293FT cells. LNCaP cells were infected with lentivirus and selected in Blasticidin (2 μ g/ml) for 2 weeks. RNAs and protein lysates were prepared from LNCaP and LNCaP

Si-FGFR-4 cells, and were used for real-time PCR and Western Blot.

Cell Adhesion Assay

For cell-substrate adhesion assay, 6-well plates coated with collagen IV were purchased from BD Biosciences. Transfected (5×10^5) PNT1a or LAPC4 cells were seeded to each well, after incubating at 37°C for 1 hr, non-adherent cells were removed by washing with PBS. Adherent cells were incubated for another 2 hr before counting. Experiments were done in triplicate and repeated three times.

RESULTS

Expression Level of Ehm2 in Immortalized Prostate Epithelial Cells and Prostate Cancer Cell Lines

To determine whether Ehm2 expression is increased in prostate cancer, we initially carried out the quantitative real-time PCR analysis using reverse transcribed RNAs from an immortalized cell line derived from benign prostatic epithelial cells (PNT1a) and three prostate cancer cell lines (PC-3, LNCaP, and LAPC4). Compared to PNT1a, higher levels of Ehm2 mRNA expression could be detected in all three prostate cancer cell lines, with the strongest expression in the androgen dependent, androgen receptor expressing LNCaP and LAPC4 cells (Fig. 1A). To confirm these findings at the protein level, we performed Western blots on protein extracts of these same four cell lines using an anti-Ehm2 antibody. A single band of approximately 43 kDa was seen in all four cell lines. This band was not seen in blots using antibody pre-incubated with the immunizing peptide (data not shown). The band is smaller than the predicted size of the full-length Ehm2 protein (57 kDa), implying the possibility of alternative translation initiation or other post-transcriptional events resulting in a smaller Ehm2 protein in prostate epithelial cells. Longer exposures of Western blots of LAPC4 and LNCaP cells revealed a weak band of approximately 57 kDa, consistent with the full length form of Ehm2 (Fig. 1C). The longer and shorter forms of Ehm2 seen in the prostate cancer cell lines on Western blots with anti-Ehm2 antibody comigrated with full length and truncated Ehm2 transiently transfected into 293T cells and detected by anti-Flag antibody directed against a Flag-epitope engineered into these constructs. It should be noted that the 5' portion of the Ehm2 mRNA is very GC-rich. Such GC-rich regions can be associated with stable secondary structures which in the appropriate cellular context, promote internal ribosome entry [23] that in this case could result in a truncated protein.

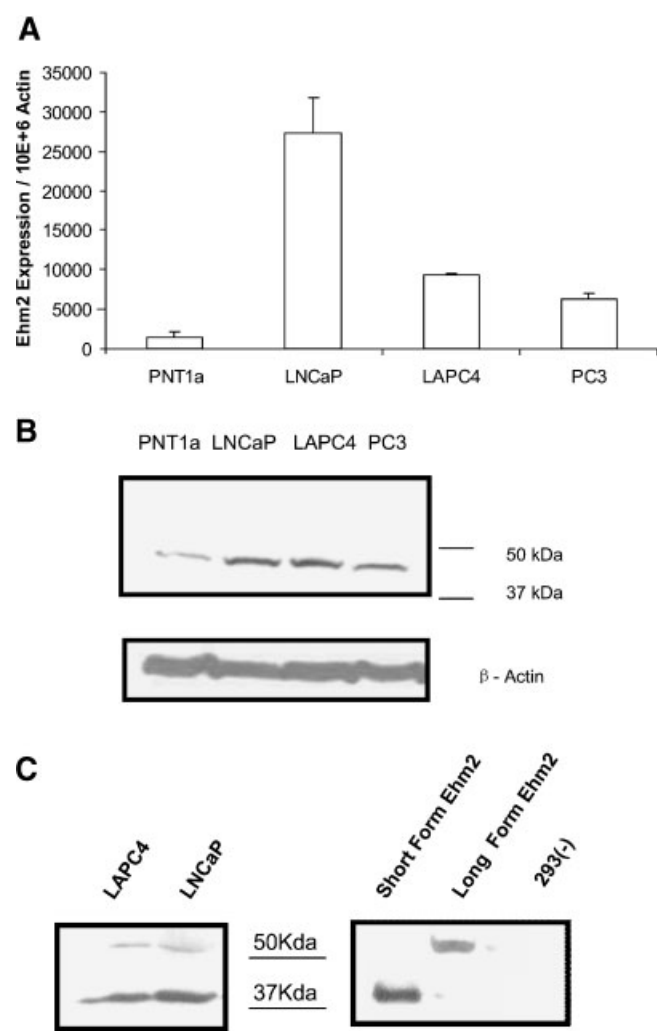


Fig. 1. Ehm2 expression in prostate cell lines. **A:** Expression of Ehm2 mRNA was determined by quantitative RT-PCR and normalized to β-actin levels and expressed as mean ± SD for duplicate experiments. PNT1a is an immortalized cell line derived from normal prostatic epithelium. LNCaP, LAPC4, and PC3 are prostate cancer cell lines. **B:** Western blot with anti-Ehm2 antibody or control anti-β-actin antibody. **C:** Longer exposure of Western blot of LAPC4 and LNCaP extracts demonstrating expression of full-length and truncated Ehm2 protein. Western blot of extracts of 293T cells transiently transfected with short or long Ehm2 cDNAs with anti-Flag antibody is shown on the left.

Localization of Expression of Ehm2 mRNA by In Situ Hybridization

To define the localization of Ehm2 mRNA in normal and cancer prostate tissues, in situ hybridization was carried out in 12 human prostate tissue samples. As shown in Figure 2, Ehm2 is expressed in normal and malignant prostatic epithelium with normal prostate epithelium showing a lower level of Ehm2 mRNA compared to the cancer epithelial cells in the same tissue (Fig. 2A, arrows). Ehm2 expression was

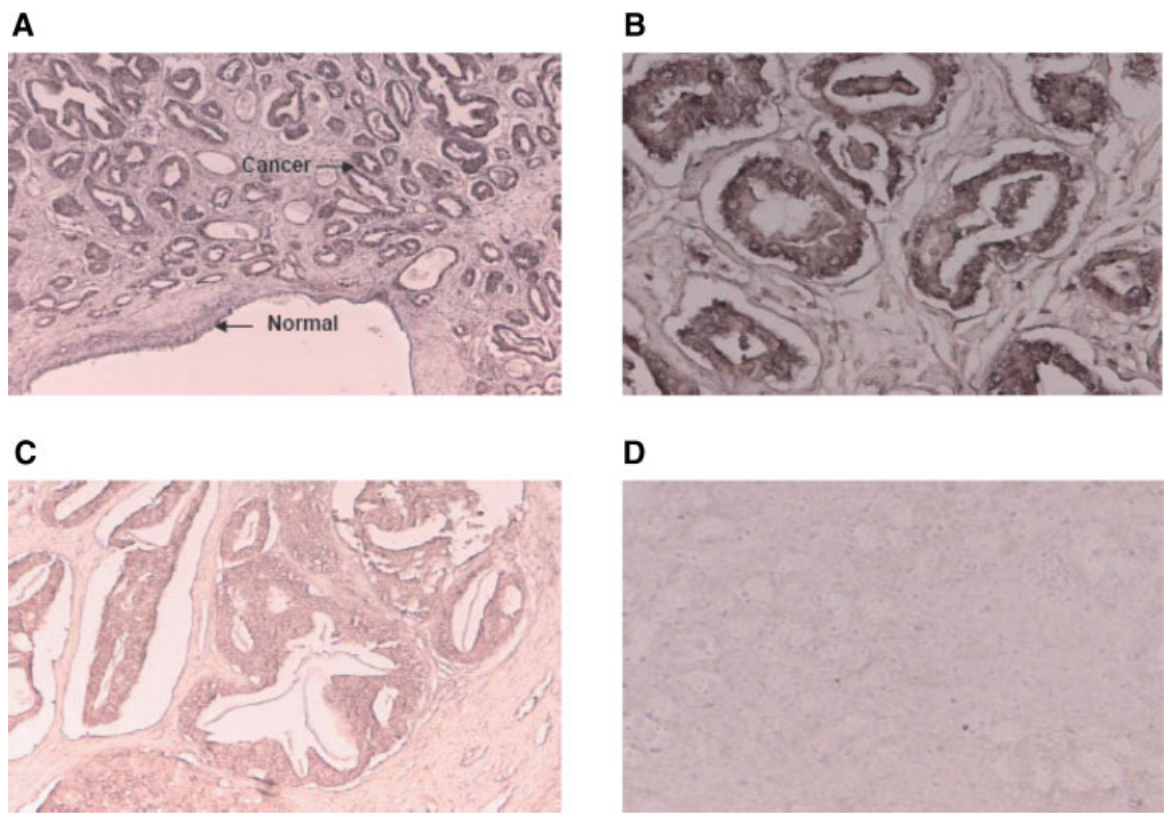


Fig. 2. Localization of Ehm2 expression in human prostate tissues using *in situ* hybridization. Ehm2 mRNA expression in human prostate tissues was determined by *in situ* hybridization as described in Materials and Methods. **A:** Prostate cancer and adjacent normal epithelium (Original magnification, $100\times$). **B:** Strong expression of Ehm2 in prostate cancer tissues ($400\times$). **C:** Moderate Ehm2 expression in prostate cancer ($100\times$). **D:** *In situ* hybridization using a sense probe of Ehm2 as a negative control ($100\times$).

predominantly in the epithelial cells of the prostate gland, with little expression in the stromal tissues (Fig. 2A). DIG-labeled sense probe of Ehm2 was used as a negative control for *in situ* hybridization and very low level of signals were detected (Fig. 2D), confirming the specificity of the *in situ* hybridization.

Determination of Ehm2 RNA Levels by Quantitative Real-Time PCR in Normal Prostate and Prostate Cancer Tissues

Our data on Ehm2 expression in cell lines indicated that Ehm2 is expressed in prostate epithelial cells and is present at higher levels in prostate cancer cells. To confirm this observation *in vivo* using a quantitative technique, we examined the Ehm2 transcript expression in 19 normal peripheral zone tissues (PZ), 8 hyperplastic transition zone samples (BPH), and 59 cancer tissues (containing at least 70% cancer) using quantitative RT-PCR. As seen in Figure 3, Ehm2 mRNA levels were about threefold higher in the cancer tissues ($5,430 \pm 1,044/10^6 \beta\text{-Actin}$; mean \pm SEM) when compared to normal peripheral zone tissues ($1,824 \pm 337/10^6 \beta\text{-Actin}$).

$10^6 \beta\text{-Actin}$). This difference was highly statically significant ($P < 0.001$, Mann–Whitney Rank Sum Test). BPH tissues showed low expression level of Ehm2 ($1,942 \pm 385/10^6 \beta\text{-Actin}$), similar to normal peripheral zone tissues. Ehm2 expression was higher in cancers from men that subsequently developed PSA recurrence, although this difference was not statistically significant.

Immunohistochemical Analysis of Ehm2 Expression Using Tissue Microarrays

To analyze expression of Ehm2 at the protein level *in vivo*, we performed immunohistochemical analysis of Ehm2 expression using a prostate cancer tissue microarray containing 32 matched normal and prostate cancer tissues (Fig. 4). Staining was almost exclusively seen in benign and malignant epithelial cells and was variable between different cases. Stained slides were digitized and scored both for extent of staining (scale of 0–3) and intensity of staining (scale of 0–3; see Materials and Methods). An average staining index was calculated from the extent of staining score for the

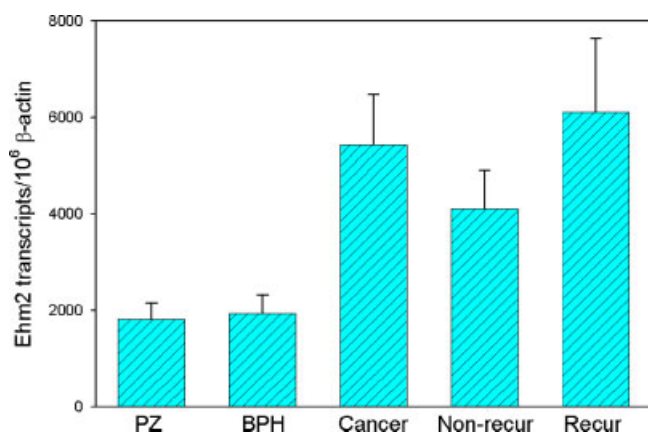


Fig. 3. Ehm2 mRNA expression in benign prostate and prostate cancer tissues as determined by quantitative real-time PCR. Expression of Ehm2 mRNA was determined by quantitative RT-PCR and normalized to β -actin levels. PZ, normal peripheral zone; BPH, hyperplastic transition zone; Cancer, all prostate cancers; Non-recr, prostate cancers with no PSA recurrence within 5 years of follow-up; Recur, prostate cancers with PSA recurrence within 5 years after radical prostatectomy. The Ehm2 expression levels are displayed as the copy number of Ehm2 transcripts per $10^6 \beta$ -actin transcripts (mean \pm standard error of the mean). The data are a representative of one of two separate experiments. [Color figure can be viewed in the online issue, which is available at www.interscience.wiley.com.]

three cores multiplied by the staining intensity score so that the staining index ranged from 0 (no staining) to 9 (extensive, strong staining). Normal prostate epithelium showed a staining index of 6.3 ± 0.38 (mean \pm SEM) while the cancer tissues had a staining index 7.4 ± 0.29 . This difference was statistically significant ($P < 0.05$, Mann-Whitney). Overall, 27% of normal tissues showed low staining (index < 6.0) while only 10% of cancers had low staining. In contrast, 40% of cancers showed maximal staining intensity (index = 9) versus 8% of normal epithelium. Of note was the finding that none of the three cancers with low Ehm2 staining (staining index < 6.0) had a PSA recurrence, while 19 of 25 cases with recurrence had moderate to strong Ehm2 staining (staining index 6–9). This difference is statistically significant ($P = 0.03$, Fisher exact test).

The FGF Receptor-4 Arg³⁸⁸ Variant Increases Ehm2 Expression

We have shown previously that prostate cancers arising in men bearing the FGFR-4 Arg³⁸⁸ polymorphic have increased rates of pelvic lymph node metastasis following radical prostatectomy [7]. To determine if Ehm2 may play a role in this increased rate of metastasis, we measured expression of Ehm2 transcripts in pooled, stably transfected PNT1a cell lines

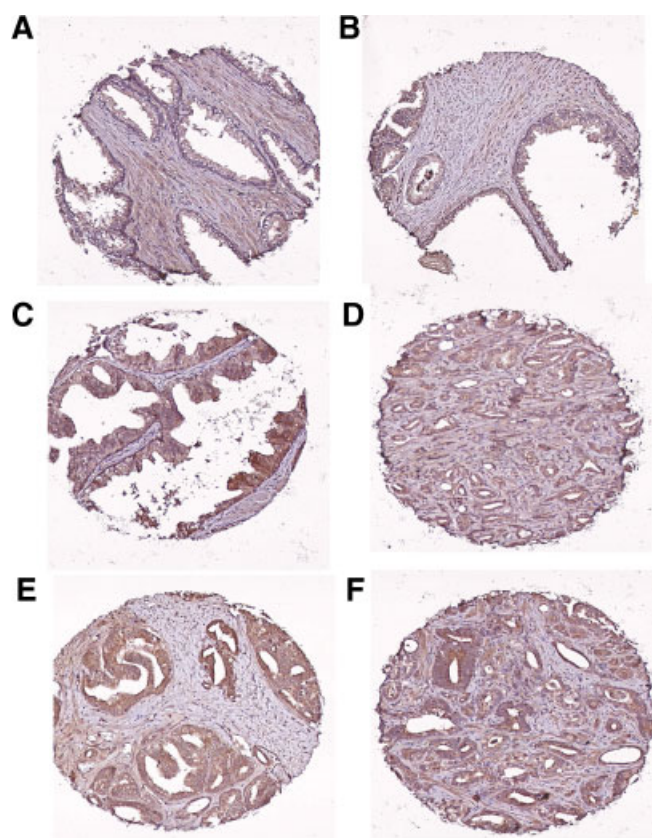


Fig. 4. Immunohistochemical determination of Ehm2 expression in prostate tissues. Tissue sections from radical prostatectomies were analyzed by immunohistochemistry with an anti-Ehm2 antibody as described in Materials and Methods using a tissue microarray. **A:** Normal prostate with weak Ehm2 staining of epithelium. Some staining of smooth muscle is also present. **B:** Normal prostate with moderate Ehm2 staining. **C:** High-grade prostatic intraepithelial neoplasia with strong Ehm2 staining. **D:** Prostate cancer with moderate Ehm2 staining. **E, F:** Prostate cancers with strong Ehm2 staining.

expressing either FGFR-4 Arg³⁸⁸ or the more common Gly³⁸⁸ variant. As described previously, these cell lines express similar levels of FGFR-4 [7]. Analysis of Ehm2 expression in these two cell lines by quantitative RT-PCR reveals that cells expressing the FGFR-4 Arg³⁸⁸ variant had 2.6-fold higher levels of Ehm2 transcripts than cells expressing the FGFR-4 Gly³⁸⁸ variant (Fig. 5A). The PNT1a cells expressing the FGFR-4 Gly³⁸⁸ variant had Ehm2 transcript levels similar to parental PNT1a cells (Fig. 1A). To confirm that Ehm2 protein levels are regulated by FGFR-4 protein, we used a SiRNA directed against FGFR-4 to downregulate FGFR-4 expression in LNCaP cells which have an Arg³⁸⁸/Gly³⁸⁸ heterozygous genotype. Western blots of protein extracts after transfection with the FGFR-4 SiRNA show marked decreases in both FGFR-4 and Ehm2 RNA and protein expression (Fig. 5B).

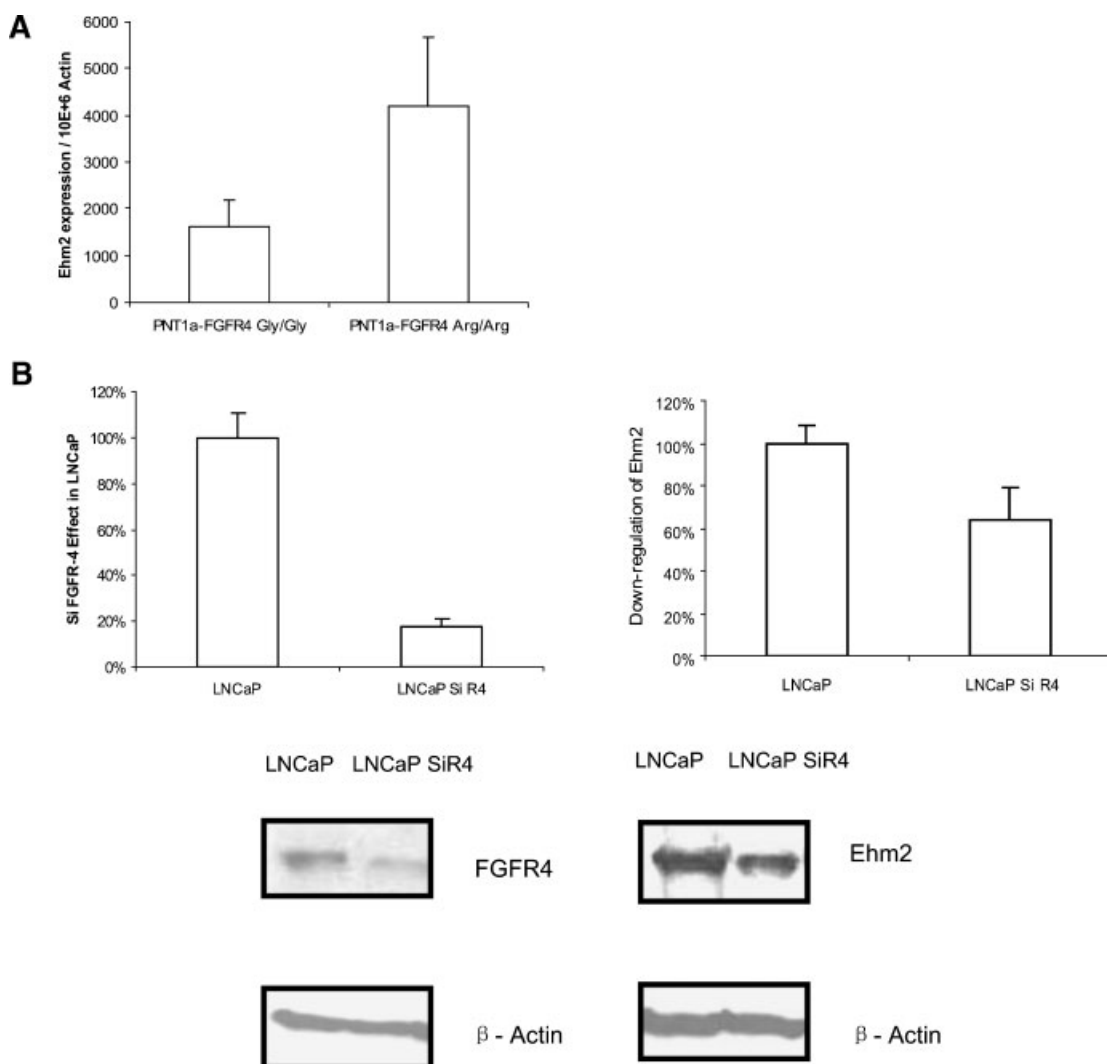


Fig. 5. Regulation of Ehm2 expression by FGFR-4 Arg³⁸⁸. **A:** Expression of Ehm2 mRNA was determined by quantitative RT-PCR and normalized to β -actin levels in RNAs from PNT1a cells overexpressing either the FGFR-4 Arg³⁸⁸ or Gly³⁸⁸ variant. Values are mean \pm SD for duplicate experiments. **B:** Expression of FGFR-4 and Ehm2 mRNA and protein as determined by quantitative RT-PCR (mean \pm SD) and Western blots in cells stably transduced with a FGFR-4 SiRNA.

Thus, FGFR-4 Arg³⁸⁸ expression results in increased expression of Ehm2.

Expression of Ehm2 Is Increased by Androgens

Based on the observation that androgens can increase expression of Ehm2 in other cell lines [16,24], and the observed higher expression of Ehm2 in androgen receptor expressing prostate cancer cell lines (Fig. 1), we tested whether there was a similar modulation of Ehm2 expression in prostate cancer cells. As shown in Figure 6, androgen treatment resulted in a twofold increase in Ehm2 transcript levels in both LNCaP and LAPC4 cells within 8–24 hr after treatment of these androgen receptor expressing cells with androgen.

Ehm2 Expression Modulates Cell Adhesion to Collagen IV

Ehm2 may regulate cytoskeleton interactions with transmembrane proteins and thus affect cancer cell adhesion [15]. In particular, alterations of FGFR-4 have been linked to decreased collagen IV adhesion in other tumors [24]. To evaluate the impact of Ehm2 on collagen IV adhesion, we carried out two series of complementary experiments. PNT1a cells, which express low levels of Ehm2, were transiently transfected with an expression vector containing the full length Ehm2 cDNA. Expression of Ehm2 was increased eightfold in the transfected cells and this was associated with a $24 \pm 2.7\%$ (mean \pm SEM, $n = 3$) decrease in adhesion to collagen IV (Fig. 7A). Since the smaller

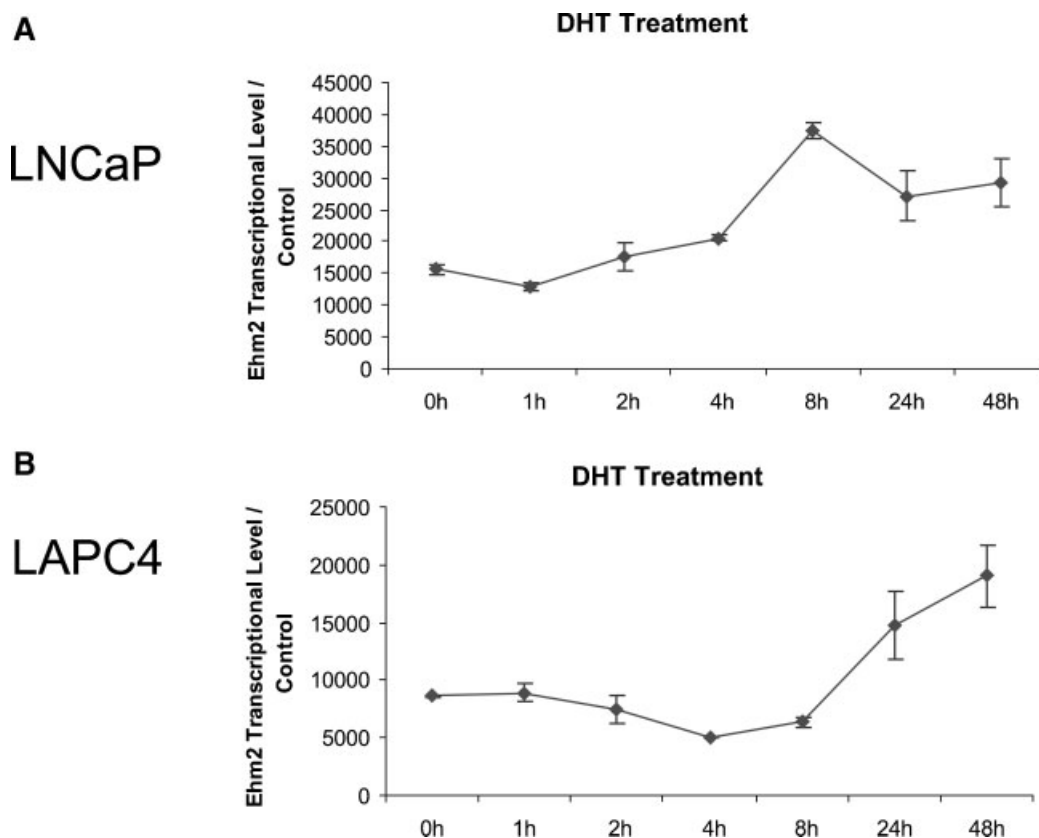


Fig. 6. Ehm2 expression can be induced by androgens. LNCa(A) and LAPC(B) cells were grown in media with charcoal stripped serum for 24 hr, then cells were refed with media containing 10 nM DHT. Cells were collected at the indicated times, with media changed at 24 hr. Ehm2 RNA levels were determined by quantitative RT-PCR and normalized to β -actin expression. Values are mean \pm SD for duplicate experiments.

form of the Ehm2 protein is the predominant form expressed in prostate cancer, we transiently expressed a truncated cDNA expressing only the smaller Ehm2 protein in PNT1a cells. Expression of this shorter form resulted in similar decrease in collagen IV adhesion ($26.3 \pm 1.3\%$, mean \pm SEM, $n = 3$). We then decreased Ehm2 mRNA in the LAPC4 cell line, which showed the second strongest Ehm2 expression among tested prostate cell lines, using a mixed SiRNA directed against the 5' portion of Ehm2. As shown in Figure 7B, 24 hr after SiRNA transfection, Ehm2 expression showed an approximately 50% decrease in Ehm2 transcript level, while adhesion to collagen IV increased $19 \pm 0.9\%$ (mean \pm SEM, $n = 3$) compared to control cells. These results indicate that increased Ehm2 expression is associated with decreased adhesion of prostatic epithelial cells to collagen IV.

DISCUSSION

The *Ehm2* gene was originally identified by differential display analysis as a gene that was upregulated in more highly metastatic clones of K-1735 and B16 murine melanoma cells [14,15]. Structural analysis of

Ehm2 revealed a FERM domain (F for 4.1 protein, E for ezrine, R for radixin, and M for moesin), which is highly conserved among different species and has been shown to be involved in the linkage of cytoplasmic proteins to the membrane [26]. For example, the cytoskeletal protein talin contains a FERM domain which plays an important role in integrin activation [27–29]. The related ERM proteins play a role in the interaction of transmembrane proteins such as ICAMs and CD44 with the actin cytoskeleton [26]. Other FERM domain proteins are cell signaling proteins such as tyrosine phosphatases [30] and focal adhesion kinase [31]. FERM domain proteins, such as NF2, can act as tumor suppressor genes [32] while others, such as URP1, are upregulated in cancer [33] and may play a role in tumor progression. Thus, FERM domain proteins can mediate a variety of critical processes at the cell membrane and may play a role as both repressors and promoters of tumor initiation and progression. Interestingly, the *Drosophila* ortholog of Ehm2, called Yurt [34], has been shown to be required for epithelial cell migration during embryogenesis, suggesting that its mammalian homolog may play a role in cancer metastasis by altering cell migratory

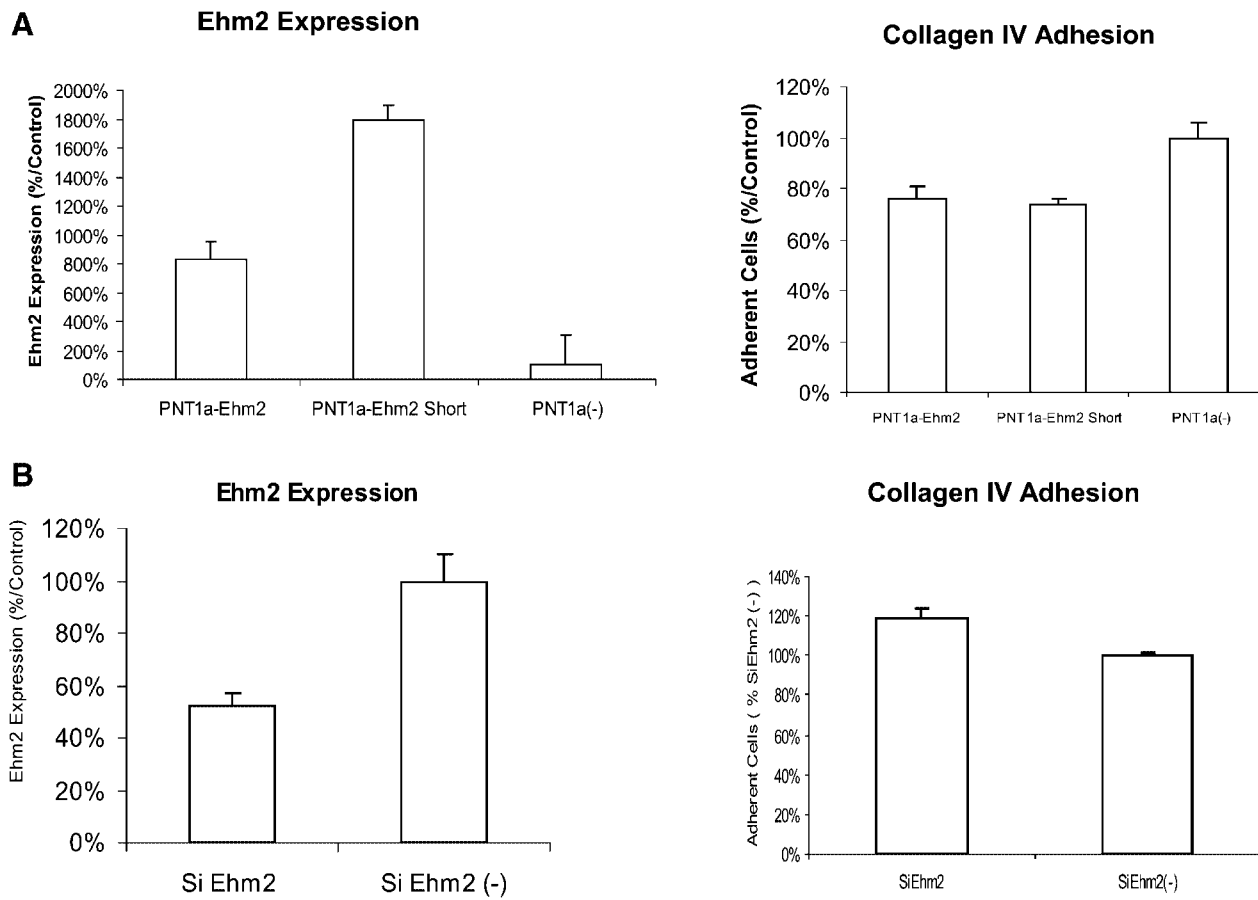


Fig. 7. Ehm2 and collagen IV adhesion. **A:** Effects of overexpression of Ehm2 in PNT1a cells on collagen IV adhesion. PNT1a cells were transiently transfected with Ehm2 cDNA or empty vector (pCEP4). Ehm2 expression was determined by quantitative RT-PCR of RNAs extracted 24 hr after transfection. Range of triplicate determinations is shown. Transfected cells were plated on collagen IV coated plates and adhesion determined as described in Materials and Methods. Adhesion is expressed as percentage of control. **B:** Effect of downregulation of Ehm2 expression in LAPC4 cells on collagen IV adhesion. LAPC4 cells were transiently transfected with Ehm2 SiRNA mixture or mock transfected. Ehm2 expression was determined by quantitative RT-PCR of RNAs extracted 24 hr after transfection. Range of triplicate determinations is shown. Transfected cells were plated on collagen IV-coated plates and adhesion determined as described in Materials and Methods. Adhesion is expressed as percentage of control.

properties. However, the biological function of Ehm2 in human prostate cells is unknown.

We have found that Ehm2 is expressed in normal prostate, prostate cancer, and cell lines derived from either normal or malignant prostate epithelial cells. Chauhan et al. [16] have previously reported expression of Ehm2 in normal prostate by Northern blotting, consistent with our observations. Based on *in situ* hybridization and immunohistochemistry, Ehm2 is expressed almost exclusively in luminal epithelial cells and cancer cells in the prostate, which is consistent with it being an androgen-regulated target gene [16,25]. We found by quantitative RT-PCR and immunohistochemistry, that Ehm2 is expressed at higher levels in prostate cancer cells. Low Ehm2 expression by immunohistochemistry was associated with decreased risk of biochemical recurrence. Such biochemical recurrence is associated with development of metastasis and death

from prostate cancer in a significant fraction of cases, while almost all men without evidence of PSA recurrence within 5 years of radical prostatectomy will remain disease-free [35]. Thus, Ehm2 is expressed at higher levels in prostate cancer and higher expression is associated with more aggressive disease.

We have shown previously that prostate cancer arising in men with a germline polymorphism of FGFR-4, which results in substitution of arginine for glycine at amino acid 388, is significantly more aggressive in that these men have higher rates of pelvic lymph node metastasis and biochemical recurrence and increased invasiveness *in vitro*. We report here that the FGFR-4 Arg³⁸⁸ polymorphism is specifically associated with increased Ehm2 expression. At least part of the increased aggressiveness of prostate cancers expressing the FGFR-4 Arg³⁸⁸ variant may be due to increased Ehm2 expression in these cancers. Our

studies indicate that Ehm2 expression can decrease adhesion to collagen IV. The degree of loss of adhesiveness is correlated with metastatic ability in some cancers. For example, in breast cancer decreased adhesion of primary breast cancer cells to collagen IV and other matrix proteins was significantly associated with lymph node metastasis [36]. The decrease in collagen IV adhesion in cells expressing Ehm2 is thus consistent with the more aggressive clinical behavior of prostate cancer cells expressing higher levels of Ehm2.

Ezzat et al. [24] have reported that a cytoplasmic FGFR-4 variant arising from a cryptic promoter (ptd-FGFR-4) is expressed in pituitary adenomas and that expression of this variant resulted in increased invasiveness of pituitary cells. Expression of the ptd-FGFR-4 variant decreased adhesion to collagen IV in pituitary cells and NIH3T3 fibroblasts compared to full length FGFR-4 in a ligand independent manner. These authors provide evidence that expression of the variant FGFR-4 leads to disruption of formation of NCAM and N-cadherin complexes in pituitary cells which could affect adhesion to collagen IV. On the other hand, Coppolino and Dedhar [37] have shown that inhibition of mitogen-activated protein kinase enhances PC3 cell attachment to collagen IV, implying that altered signal transduction from growth factor receptors can modulate collagen IV adhesion. Clearly, further mechanistic studies are needed of the role of FGFR-4 in cell adhesion and the possible participation of Ehm2 in this process. However, the finding of both increased invasiveness and decreased collagen IV adhesion in pituitary cells expressing the ptd-FGFR-4 variant has clear parallels to our findings regarding the FGFR-4 Arg³⁸⁸ variant and Ehm2 in prostate cancer.

Based on our studies, expression of Ehm2 is controlled by multiple factors. On average, both in vitro and in vivo, transformed prostatic epithelial cells express two- to threefold higher levels of Ehm2 than untransformed cells. In addition, androgen can induce Ehm2 approximately twofold in androgen receptor expressing prostate cancer cells. Finally, the presence of the FGFR-4 Arg³⁸⁸ variant is also associated with two- to threefold increase in Ehm2 expression. The mechanism(s) by which FGFR-4 Arg³⁸⁸ and androgen can induce Ehm2 mRNA expression is unclear. There are indications that these mechanisms may be additive. Comparing the expression of Ehm2 in the androgen receptor expressing cell lines, the LNCaP cell line has an Arg³⁸⁸/Gly³⁸⁸ genotype and has a 2.5-fold higher expression of Ehm2 compared to LAPC4, which has a Gly³⁸⁸/Gly³⁸⁸ genotype. Similarly, for the AR negative cell lines, PC3, which has an Arg³⁸⁸/Arg³⁸⁸ genotype, expresses 2.1-fold more Ehm2 than DU145, which has a Gly³⁸⁸/Gly³⁸⁸ genotype. Detailed studies of the underlying mechanisms, either direct or indirect, that

control expression Ehm2 in response to androgens and FGFR-4 expression are clearly needed.

In summary, Ehm2 is increased in prostate cancer and higher expression is associated with increased risk of biochemical recurrence following radical prostatectomy. Concordant with this finding, Ehm2 expression is increased in prostate cells expressing the FGFR-4 Arg³⁸⁸ variant, which is also associated with biochemical recurrence. At the cellular level, increased Ehm2 expression results in decreased adhesion of cells to collagen IV. Further mechanistic studies defining the molecular mechanisms controlling Ehm2 expression and its role in cell adhesion are needed to clarify the role of this protein in the progression of prostate cancer.

ACKNOWLEDGMENTS

This work was supported by the use of the facilities of the Michael E. DeBakey VAMC, the Department of Veterans Affairs Merit Review program (M.I.), and through the generous support of the Jack Findlay Doyle II Charitable Fund (R.L.M.).

REFERENCES

- Jemal A, Tiwari RC, Murray T, Ghafoor A, Samuels A, Ward E, Feuer E J, Thun MJ. Cancer statistics, 2004. CA Cancer J Clin 2004;54:8–29.
- Thompson TC. Metastasis-related genes in prostate cancer: The role of caveolin-1. Cancer Metastasis Rev 1998;17:439–442.
- Bangma CH, Nasu Y, Ren C, Thompson TC. Metastasis-related genes in prostate cancer. Semin Oncol 1999;26:422–427.
- Jaeger EB, Samant RS, Rinker-Schaeffer CW. Metastasis suppression in prostate cancer. Cancer Metastasis Rev 2001;20:279–286.
- Kauffman EC, Robinson VL, Stadler WM, Sokoloff MH, Rinker-Schaeffer CW. Metastasis suppression: The evolving role of metastasis suppressor genes for regulating cancer cell growth at the secondary site. J Urol 2003;169:1122–1133.
- Tricoli JV, Schoenfeldt M, Conley BA. Detection of prostate cancer and predicting progression: Current and future diagnostic markers. Clin Cancer Res 2004;10:3943–3953.
- Wang J, Stockton DW, Ittmann M. The fibroblast growth factor receptor-4 Arg388 allele is associated with prostate cancer initiation and progression. Clin Cancer Res 2004;10:6169–6178.
- Kwabi-Addo B, Ozen M, Ittmann M. The role of fibroblast growth factors and their receptors in prostate cancer. Endocr Relat Cancer 2004;11:709–724.
- Bange J, Precht D, Cheburkin Y, Specht K, Harbeck N, Schmitt M. Cancer progression and tumor cell motility are associated with the FGFR4 Arg (388) allele. Cancer Res 2002;62:840–847.
- Morimoto Y, Ozaki T, Ouchida M, Umehara N, Ohata N, Yoshida A, Shimizu K, Inoue H. Single nucleotide polymorphism in fibroblast growth factor receptor 4 at codon 388 is associated with prognosis in high-grade soft tissue sarcoma. Cancer 2003;98:2245–2250.
- Streit S, Bange J, Fichtner A, Ihrler S, Issing W, Ullrich A. Involvement of the FGFR4 Arg388 allele in head and neck squamous cell carcinoma. Int J Cancer 2004;111:213–217.

12. Jezequel P, Campion L, Joalland MP, Millour M, Dravet F, Classe JM, Delecroix V, Deporte R, Fumoleau P, Ricolleau G. G388R mutation of the FGFR4 gene is not relevant to breast cancer prognosis. *Br J Cancer* 2004;90:189–193.
13. Spinola M, Leoni VP, Tanuma J, Pettinicchio A, Frattini M, Signoroni S, Agresti R, Giovanazzi R, Pilotti S, Bertario L, Ravagnani F, Dragani TA. FGFR4 Gly388Arg polymorphism and prognosis of breast and colorectal cancer. *Oncol Rep* 2005;14:415–419.
14. Shimizu K, Nagamachi Y, Tani M, Kimura K, Shiroishi T, Wakana S, Yokota J. Molecular cloning of a novel NF2/ERM/4.1 superfamily gene, ehm2, that is expressed in high-metastatic K1735 murine melanoma cells. *Genomics* 2000;65:113–120.
15. Hashimoto Y, Shindo-Okada N, Tani M, Takeuchi K, Toma H, Yokota J. Identification of genes differentially expressed in association with metastatic potential of K-1735 murine melanoma by messenger RNA differential display. *Cancer Res* 1996;56:5266–5271.
16. Chauhan S, Pandey R, Way JF, Sroka TC, Demetriou MC, Kunz S, Cress AE, Mount DW, Miesfeld RL. Androgen regulation of the human FERM domain encoding gene EHM2 in a cell model of steroid-induced differentiation. *Biochem Biophys Res Commun* 2003;310:421–432.
17. Pang ST, Dillner K, Wu X, Pousette A, Norstedt G, Flores-Morales A. Gene expression profiling of androgen deficiency predicts a pathway of prostate apoptosis that involves genes related to oxidative stress. *Endocrinology* 2002;143:4897–4906.
18. Yu Y, Khan J, Khanna C, Helman L, Meltzer PS, Merlino G. Expression profiling identifies the cytoskeletal organizer ezrin and the developmental homeoprotein Six-1 as key metastatic regulators. *Nat Med* 2004;10:175–181.
19. Klein KA, Reiter RE, Redula J, Moradi H, Zhu XL, Brothman AR, Lamb DJ, Marcelli M, Belldegrun A, Witte ON, Sawyers CL. Progression of metastatic human prostate cancer to androgen independence in immunodeficient SCID mice. *Nat Med* 1997;3:402–408.
20. Wheeler TM, Lebovitz RM. Fresh tissue harvest for research from prostatectomy specimens. *Prostate* 1994;25:274–279.
21. Weng J, Wang J, Cai Y, Stafford L, Mitchell D, Ittmann M, Liu M. Increased expression of prostate-specific G-protein coupled receptor (PSGR) in human prostate intraepithelial neoplasia (PIN) and prostate cancers. *Int J Cancer* 2004;113:811–818.
22. Kwabi-Addo B, Wang J, Erdem H, Vaid A, Castro P, Ayala G, Ittmann M. Expression of Sprouty1, an inhibitor of fibroblast growth factor signal transduction, is decreased in human prostate cancer. *Cancer Res* 2004;64:4728–4735.
23. Pickering M, Willis A. The implications of structured 5 untranslated regions on translation and disease. *Semin Cell Develop Biol* 2005;16:39–47.
24. Ezzat S, Zheng L, Asa SL. Pituitary tumor-derived fibroblast growth factor receptor 4 isoform disrupts neural cell-adhesion molecule/N-cadherin signaling to diminish cell adhesiveness: A mechanism underlying pituitary neoplasia. *Mol Endocrinol* 2004;18:2543–2552.
25. Chauhan S, Kunz S, Davis K, Roberts J, Martin G, Demetriou MC, Sroka TC, Cress AE, Miesfeld RL. Androgen control of cell proliferation and cytoskeletal reorganization in human fibrosarcoma cells: Role of RhoB signaling. *J Biol Chem*. 2004;279:937–944.
26. Chishti AH, Kim AC, Marfatia SM, Lutchman M, Hanspal M, Jindal H, Liu SC, Low PS, Rouleau GA, Mohandas N, Chasis JA, Conboy JG, Gascard P, Takakuwa Y, Huang SC, Benz EJ Jr, Bretscher A, Fehon RG, Gusella JF, Ramesh V, Solomon F, Marchesi VT, Tsukita S, Tsukita S, Arpin M, Louvard D, Tonks N, Anderson J, Fanning A, Bryant P, Woods D, Hoover KB. The FERM domain: A unique module involved in the linkage of cytoplasmic proteins to the membrane. *Trends Biochem Sci*. 1998;23:281–282.
27. Lee HS, Bellin RM, Walker DL, Patel B, Powers P, Liu H, Garcia-Alvarez B, de Pereda JM, Liddington RC, Volkmann N, Hanein D, Critchley DR, Robson RM. Characterization of an actin-binding site within the talin FERM domain. *J Mol Biol* 2004;343:771–784.
28. Campbell ID, Ginsberg MH. The talin-tail interaction places integrin activation on FERM ground. *Trends Biochem Sci* 2004;29:429–435.
29. Calderwood DA. Talin controls integrin activation. *Biochem Soc Trans* 2004;32:434–437.
30. Bompard G, Martin M, Roy C, Vignon F, Freiss G. Membrane targeting of protein tyrosine phosphatase PTPL1 through its FERM domain via binding to phosphatidylinositol 4,5-biphosphate. *J Cell Sci* 2003;116:2519–2530.
31. Dunty JM, Gabarra-Niecko V, King ML, Ceccarelli DF, Eck MJ, Schaller MD. FERM domain interaction promotes FAK signaling. *Mol Cell Biol* 2004;24:5353–5368.
32. Johnson KC, Kissil JL, Fry JL, Jacks T. Cellular transformation by a FERM domain mutant of the Nf2 tumor suppressor gene. *Oncogene* 2002;21:5990–5997.
33. Weinstein EJ, Bourner M, Head R, Zakeri H, Bauer C, Mazzarella R. URP1: A member of a novel family of PH and FERM domain-containing membrane-associated proteins is significantly overexpressed in lung and colon carcinomas. *Biochim Biophys Acta* 2003;1637:207–216.
34. Hoover KB, Bryant PJ. Drosophila Yurt is a new protein-4.1-like protein required for epithelial morphogenesis. *Dev Genes Evol*. 2002;212:230–238.
35. Pound CR, Partin AW, Eisenberger MA, Chan DW, Pearson JD, Walsh PC. Natural history of progression after PSA elevation following radical prostatectomy. *JAMA* 1999;281:1591–1597.
36. Gui GP, Puddefoot JR, Vinson GP, Wells CA, Carpenter R. Altered cell-matrix contact: A prerequisite for breast cancer metastasis? *Br J Cancer* 1997;75:623–633.
37. Coppolino MG, Dedhar S. Ligand-specific, transient interaction between integrins and calreticulin during cell adhesion to extracellular matrix proteins is dependent upon phosphorylation/dephosphorylation events. *Biochem J* 1999;340: 41–50.

Altered fibroblast growth factor receptor-4 trafficking promotes prostate cancer progression

Jianghua Wang, Wendong Yu, Yi Cai, Chengxi Ren and Michael Ittmann

Dept. of Pathology of Baylor College of Medicine and Michael E. DeBakey Dept. of Veterans Affairs Medical Center, Houston, Texas 77030.

Running Title: Altered FGFR-4 trafficking and prostate cancer progression

Key Words: prostate cancer, fibroblast growth factor receptor, receptor trafficking, signal transduction, polymorphism

Grant Support: Dept of Veterans Affairs Merit Review program (MI), the Dept of Defense Prostate Cancer Research Program (W81XWH-04-1-0843), the National Cancer Institute to the Baylor prostate cancer SPORE program (P50CA058204) and the and by use of the facilities of the Michael E. DeBakey Dept. of Veterans Affairs Medical Center

Correspondence:

Michael Ittmann MD/PhD
Department of Pathology
Baylor College of Medicine
One Baylor Plaza Houston, TX 77030
Tele: (713) 798-6196
Fax: (713) 798-5838
E-mail: mittmann@bcm.tmc.edu

ABSTRACT

Fibroblast growth factor receptor-4 (FGFR-4) is expressed at significant levels in almost all human prostate cancers and expression of FGFR-4 ligands is ubiquitous. A common polymorphism of FGFR-4 in which arginine (Arg³⁸⁸) replaces glycine (Gly³⁸⁸) at amino acid 388 is associated with progression in human prostate cancer. We show that the FGFR-4 Arg³⁸⁸ polymorphism, which is present in the majority of prostate cancer patients, results in increased receptor stability and sustained receptor activation. In patients bearing the FGFR-4 Gly³⁸⁸ variant, expression of Huntington-interacting protein 1 (HIP1), which occurs in more than half of human prostate cancers, also results in FGFR-4 stabilization and sustained activation. This is associated with enhanced proliferation and anchorage independent growth *in vitro*. Our findings indicate that increased receptor stability and sustained fibroblast growth factor receptor-4 signaling occur in the majority of human prostate cancers due to either the presence of a common genetic polymorphism or expression of a protein which stabilizes FGFR-4. Both of these alterations are associated with clinical progression in patients with prostate cancer. Thus FGFR-4 signaling and receptor turnover are important potential therapeutic targets in prostate cancer.

INTRODUCTION

Prostate cancer is the most common cancer and the second leading cause of cancer deaths in US men(1) . Multiple genetic and epigenetic alterations have been described in prostate cancer which can promote initiation and progression of this disease. Prominent among these changes are alterations in the fibroblast growth factor signaling pathway (for review see Kwabi-Addo et al (2)). The fibroblast growth factor (FGF) gene family consists of 22 different genes encoding related polypeptide mitogens. FGFs have a broad range of biological activities which can play an important role in tumorigenesis including promotion of proliferation, motility and angiogenesis and inhibition of cell death (2-4). It is well established that multiple FGF receptor ligands, including FGF1 (5), FGF2 (6, 7), FGF6 (8), FGF8 (9, 10) and FGF17 (11), are increased in prostate cancer and, based on correlations with clinical and pathological parameters, appear to play a role in prostate cancer progression.

FGFs interact with a family of four distinct, high affinity tyrosine kinase receptors, designated FGFR1-4 (for review see (3)). These receptors consist of an extracellular portion containing 3 immunoglobulin-like domains and an intracellular tyrosine kinase domain and have variable affinities for the different FGFs. Ultimately, activation of FGF receptors leads to signal transduction through multiple pathways, including PLC γ , phosphatidylinositol 3-kinase, mitogen-activated protein kinases and STATs (2, 3, 12). These effectors, in turn, disseminate the receptor tyrosine kinase signals by activating many additional target proteins. All of these pathways have been shown to be upregulated in prostate cancer and each of these pathways contributes to prostate cancer initiation and progression (2).

There is now clear-cut evidence for the involvement of FGFR-4 in prostate cancer initiation and progression. All of the FGFs which are increased in human prostate cancer tissues are potent activators of FGFR-4. Our group (13) and others (14, 15) have shown increased expression of FGFR-4 in prostate cancer by quantitative RT-PCR and immunohistochemistry.

Strong expression of FGFR-4 in prostate cancer cells, as assessed by immunohistochemistry, is significantly associated with increased clinical stage and tumor grade and decreased patient survival (14). Based on these studies it is clear that FGFR-4 is expressed in almost all human prostate cancers.

A germline polymorphism in the FGFR-4 gene, resulting in expression of FGFR-4 containing either glycine (Gly^{388}) or arginine (Arg^{388}) at codon 388 was identified several years ago and the presence of the FGFR-4 Arg^{388} allele was associated with decreased disease free survival in breast cancer patients with lymph node metastasis as well as with metastasis and poor prognosis in colon cancer (16). Since the initial report, further studies in a variety of malignancies, including soft tissue sarcomas (17), melanoma (18), lung adenocarcinoma (19) and head and neck squamous cell carcinoma (20, 21) have linked the presence of the FGFR-4 Arg^{388} allele with aggressive disease and adverse clinical outcomes. There have been some discordant reports regarding the role of the FGFR-4 Arg^{388} in breast cancer (22), but this may be explained by differences in treatment regimen, since recent studies indicate that the FGFR-4 Arg^{388} polymorphism modulates response to chemotherapy (23). We have found that the presence of homozygosity for the FGFR-4 Arg^{388} allele is significantly associated with prostate cancer incidence in white men (13). Furthermore, the presence of the FGFR-4 Arg^{388} polymorphism is correlated with the occurrence of pelvic lymph node metastasis and biochemical (PSA) recurrence in men undergoing radical prostatectomy (13). Expression of the FGFR-4 Arg^{388} variant results in increased cell motility and invasion as well as upregulation of genes such as uPAR (13) and Ehm2 (24), which are known to promote invasion and metastasis. These *in vitro* observations may explain, in part, the increased aggressiveness of prostate cancer in men bearing this polymorphism. This polymorphism is very prevalent in the white (Caucasian) population since approximately 45% of individuals are hetero- or homozygous for this allele in all white populations studied to date.

While the expression of the FGFR-4 Arg³⁸⁸ variant is associated with prostate cancer initiation and aggressive disease, an important question remains: what is the molecular basis for the difference between the two FGFR-4 variants? Achondroplasia is caused by a similar mutation in FGFR-3 (Gly³⁸⁰ to Arg³⁸⁰). Increased FGFR-3 signaling due to this mutation inhibits proliferation in chondrocytes (25, 26) and hence the phenotype. Elegant studies have shown that this mutation leads to decreased receptor turnover due to increased receptor recycling and decreased targeting of receptors to lysosomes (25, 26). We therefore sought to determine if a similar phenomenon occurs with the FGFR-4 Arg³⁸⁸ variant. In addition, we have begun to investigate other proteins that can potentially modulate FGFR-4 receptor trafficking. One such protein is HIP1 (Huntingtin interacting protein 1). HIP1 can interact with clathrin as well alpha-adaptin, which is part of the AP-2 late endocytic complex (27). It has been shown that HIP1 can stabilize EGF receptors (27, 28) and the primary site of such stabilization appears to be via stabilization in early endosomes (27). Over-expression of HIP1 leads to transformation of NIH3T3 cells (28). Of note, it has been shown by immunohistochemistry that there is moderate to strong expression of HIP1 in about 50% of clinically localized prostate cancers and that absence of HIP1 expression is associated with complete absence of biochemical recurrence following radical prostatectomy (29). We report here that the FGFR-4 Arg³⁸⁸ variant has markedly decreased degradation and increased phosphorylation following ligand binding when compared to the Gly³⁸⁸ variant. On the other hand, interaction with HIP1 stabilizes the FGFR-4 Gly³⁸⁸ variant and results in increased proliferation and soft agar colony formation. Thus altered FGFR-4 receptor trafficking is a common feature in human prostate cancer that is associated with changes in cellular behavior *in vitro* and clinical progression.

MATERIALS AND METHODS

Tissue samples and cell lines. RNAs were extracted from snap frozen cancer tissues (>70% cancer) and benign peripheral zone tissue from men undergoing radical prostatectomy as described previously (30). Clinical and pathological characteristics of these samples have been described previously (30). PNT1A, a non-tumorigenic SV40-immortalized human prostatic epithelial cell line, and the PC3, LNCaP and DU145 prostate cancer cell lines were all maintained in RPMI1640 media with 10% fetal bovine serum (FBS). 293T cells were maintained in DMEM with 10% FBS.

Si-FGFR-4 and Si-HIP1 lentivirus Lentiviruses to knock down FGFR-4 or HIP1 RNA were generated using Block-iT™ Lentiviral RNAi Expression System (Invitrogen, Carlsbad, CA). Primers used for lentiviral constructs were: Si R4 F 5'CACCGCATAGGGACCTCTCGAAT ATTGAAAAATATTCGAGAGGGTCCCTATGC-3' Si R4 R 5'AAAAGCATAGGGACCTCTC GAATAT TTT CG AA TA TTCGAGA GGTCCCT ATGC-3'SiHIP1F: 5'- CACCGGACTCA GACTGTCAGCATCGATGCTGACAGTCTGAGTCC -3'SiHIP1R: 5'- AAAAGG ACT CAGACTGTCAGCATCGATGCTGACAGTCTGAGTCC -3'. Lentiviral constructs were generated according to manufacturer's instruction using 293FT cells. Following infection with lentivirus, cells were selected in Blasticidin (2μg/ml) containing media. RNAs was extracted from pooled cells and mRNAs levels of target genes quantitated by quantitative RT-PCR.

Expression vector cloning, transfection and stable selection. The full length FGFR-4 Gly³⁸⁸ and Arg³⁸⁸ isoforms, were obtained from DU145 and PC3 cell line cDNAs respectively, and cloned into Topo-V5 expression vector (Invitrogen) by using primers of FGFR-4 Exp F: 5'- CCT GAGAGCTGTGAGAAG G-3' and FGFR-4 Exp R: 5'-GGATCCAGCTCCTCCCC-3'. Annealing temperature is 60°C. HIP1 constructs were cloned into pCMV-Tag2B expression vector (Stratagene, LaJolla, CA), which has a Flag Tag at N terminal in frame. The full-length HIP1 and N-terminal truncated HIP1(-183) sequences were obtained from PNT1a cell line cDNA by RT-PCR using primers with a 5' Sall cutting site and a 3' Xhol site. Primers were: HIP1 Exp F (Sall):

5'- ACGCGTCGACATGGATCGGAT G-3'; HIP1 Exp F2 (Sall): 5'-ACGCGTCGACCA GTTAACAGTGGA G -3'; HIP1 Exp R (Xhol): 5'-CCGCTCGAGTTCTTTTGGTTACCA C-3'. All constructs were sequenced to confirm the absence of mutations due to the PCR reaction and verify the accuracy of the tag sequences in frame. The expression of full length proteins were confirmed by Western blot using cell lysate from transiently transfected 293T cells overexpressing FGFR-4 or HIP1. Anti-V5 antibody (1:5000) from Invitrogen and anti-Flag antibody (1:2000) from Stratagene were used. To generate stable cell lines, 3×10^5 cells per 60-mm dish were prepared 24h before transfection. 2 μ g of plasmid was transfected with 6 μ l Fugene6 (Invitrogen) in a total volume of 4 ml of OPTI-MEM without serum. Five hours later after transfection, one ml of FBS was then added to each dish to achieve a final serum concentration of 20%. After an additional 18 hours of incubation, cells were refed with complete medium and then split 1:3 after 48 hours. The next day, selection was initiated by the addition of G418 at 200 μ g/ml. Selection was carried out for 2 weeks, and long-term cultures were routinely maintained in G418 (100 μ g/ml).

Western blot and immunoprecipitation. Total protein was extracted from cells using RIPA lysis buffer (Santa Cruz Biotechnology, Santa Cruz, CA). For Western blots, 40 μ g of protein extract/lane were electrophoresed, transferred to nitrocellulose membrane (Hybond ECL; Amersham Biosciences, Piscataway, NJ), and incubated overnight with a anti-V5 monoclonal antibody (1:5000 dilution, Invitrogen), anti-Flag M2 monoclonal antibody (1:2000 dilution, Stratagene), anti-FGFR-4 (1:500, Santa Cruz), anti-HIP1 (1:10000, Novus Biologicals, Littleton, CO) or anti- β -actin (1:5000, Sigma, St Louis, MO) . Membranes were washed and treated with mouse anti-goat IgG (1:5000; Santa Cruz) or goat anti-rabbit (1:50000, Santa Cruz) conjugated to horseradish peroxidase. The antigen-antibody reaction was visualized using an enhanced chemiluminescence (ECL) assay (Amersham Biosciences) and exposed to ECL film (Amersham Biosciences). For immunoprecipitation, 1mg of protein lysate from each sample was incubated with anti-V5 (1:500) overnight at 4°C. Tyrosine phosphorylation site detection antibody p20

(Santa Cruz) was used at 1:500 dilution.

Quantitative real-time PCR. All quantitative RT-PCR was carried out using the basic procedure described previously(30). Primers for HIP1 were located between exon 4 and 8 (Genebank access: NM_005338). HIP1 RT Forward: 5'-TGCTCTGCTGGAAGTTCTG-3'; HIP1 RT Reverse: 5'-CTGGCGGTCACTCATCTG-3'. Primers for β-Actin were as described previously (30). The plasmid concentrations were converted into copy number and a dilution series of each plasmid from 10^8 to 10^2 were used as DNA standard for real-time PCR. All real-time PCR efficiencies were controlled in the range of $100\% \pm 5$.

Receptor degradation assay. 2×10^6 293 cells were plated into each 10 cm dishes 24h before transfection. Cells were transfected with 8μg plasmid in total in each dish. 48h after transfection, cells were trypsinized and washed with ice-cold PBS three times. Cell pellets were resuspended in PBS at $\sim 2.5 \times 10^7$ / ml. 200ul 10mM biotin was added into each 1ml PBS cell suspension. After 15min incubation at $4^\circ C$, cells were washed by PBS with 100mM glycine three times. Then they were put back to culture dish at $37^\circ C$ with complete DMEM plus 100ng/ml FGF2 and 20U/ml heparin for different time period. Cells were collected at 0h, 6h, 24h and 48h and lysed with 1ml RIPA buffer with 1% Triton and sonicated. For immunoprecipitation, 60μl Streptavidin-AG beads were used for 1mg lysate of each sample, with overnight incubation at $4^\circ C$.

In vitro binding assay. To investigate which domain of HIP1 protein associates with FGFR-4, we made a series of purified HIP1 proteins with truncated domains by using Variflex Bacterial Protein Expression System (Stratagene). We used N-terminal SBP-SET2c for HIP1 proteins expression due to different enzyme cutting sites. Primers used were: HIP1 Exp F V (SmaI): 5'-TCC CCC GGG ATG GAT CGG ATG-3'; HIP1 Exp F2 V (SmaI): 5'-TCC CCC GGG CAG TTA ACA GTG G -3'; HIP1 Exp F3 V (SmaI): 5'-TCC CCC GGG GAG ATC AGT GGA TTG-3'; HIP1 Exp F4 V (SmaI): 5'-TCC CCCGGG ACTCAGCTAAA C-3'; HIP1 Exp F5 V (SmaI): 5'- TCC CCCGGGGCCAGA ATAGAG-3'; HIP1 Exp R V (XbaI): 5'-CCGCTCGAGCTA TTCTTTTC GGTTACCAC-3'. Purified proteins, dissolved in streptavidin binding buffer at 0.2ug/ul, were

verified by electrophoresis and Coomassie Blue staining before being applied to binding assay. 293T cell lysate (350ul) in RIPA buffer from cells with transient overexpression of FGFR-4 was mixed with 50ul of different purified HIP1 domain proteins. After incubation at 4°C overnight, streptavidin beads were spun down and washed three times by PBST followed by standard Western Blot by using anti-V5 antibody.

Proliferation. PNT1A or DU145 cells overexpressing HIP1 protein or vector controls were plated at 1x 10⁵/60mm dish. Cells grown in different media, complete RPMI 1640 with 10%FBS, 0.5%FBS, or 1%ITS (Sigma) plus 20ng/ml FGF2, were counted at days 2, 4, 6, and 8. Cell number was determined in triplicate using a Coulter counter.

Soft Agar Assay 35mm dishes with 0.5% base agar layer mixed with 1X culture media plus 10% FBS were prepared before the seeding of cells. 10⁵ PNT1A cells transfected with HIP1 expression vector or control were plated in 0.35% top agar layer over the base agar. Plates were stained with crystal violet and cell colonies were counted after incubation at 37°C in humidified incubator for three weeks.

RESULTS

The FGFR-4 Arg³⁸⁸ variant has decreased degradation and sustained phosphorylation following ligand stimulation compared to the Gly³⁸⁸ variant.

To assess differences in receptor degradation between the two FGFR-4 variants following ligand stimulation, we transfected 293T cells with either the Arg³⁸⁸ or Gly³⁸⁸ FGFR-4 variant, biotinylated cell surface receptors and lysed cells at intervals after ligand (FGF2) stimulation. Biotin-labeled proteins were then precipitated using streptavidin beads and the precipitates used for Western blots with anti-V5 antibody recognizing a V-5 tag on the transfected FGFR-4 variants. As can be seen in Fig 1A, the FGFR-4 Arg³⁸⁸ variant is much more stable than the Gly³⁸⁸ variant. We have repeated this experiment multiple times with essentially identical results. Thus, the FGFR-4 Arg³⁸⁸ variant is degraded much more slowly after ligand binding. To

determine if there were differences in FGFR-4 receptor phosphorylation between the two variants, we transfected 293T cells with either variant, incubated cells in media with insulin as the only growth factor for 24 hours, stimulated cells with FGF2 and collected cell lysates at intervals after ligand addition. Total FGFR-4 was then immunoprecipitated with anti-V5 antibody and tyrosine phosphorylated FGFR-4 detected by Western blot. Initial experiments revealed that the FGFR-4 Gly³⁸⁸ isoform had a peak phosphorylation at 5 minutes with a marked decrease in phosphorylation at 15 minutes after addition of ligand (Fig 1B). In contrast, the FGFR-4 Arg³⁸⁸ phosphorylation was higher at 15 minutes after ligand addition than at 5 minutes. Examination of later timepoints revealed a peak phosphorylation at 30 minutes with still substantial phosphorylation 120 minutes after ligand addition for the Arg³⁸⁸ variant (Fig 1C) while the Gly³⁸⁸ variant showed only minimal residual phosphorylation at 15 and 30 minutes and no detectable phosphorylation at 120 minutes even on long exposures (data not shown). Thus the FGFR-4 Arg³⁸⁸ variant displays increased stability and much higher levels of sustained activation than the Gly³⁸⁸ variant.

HIP1 mRNA is increased in prostate cancer and increased expression is associated with PSA recurrence following radical prostatectomy

Previous immunohistochemical studies have shown that HIP1 protein is increased in prostate cancer and that absence of HIP1 staining was associated with a favorable prognosis following radical prostatectomy (29). To confirm these findings using an alternative approach, we used quantitative RT-PCR to evaluate HIP1 mRNA expression in normal peripheral zone tissue and cancer tissue from men with no PSA recurrence within 5 years following radical prostatectomy versus men with PSA recurrence within 5 years of radical prostatectomy (Fig 2). We found that HIP1 mRNA is significantly increased in prostate cancer ($p=0.018$, Mann-Whitney Test) and is higher in cancers with biochemical recurrence following radical prostatectomy versus those with no recurrence ($p=0.05$, Mann Whitney Rank Sum Test). Thus, in agreement with prior studies,

our results indicate that HIP1 may play an important role in promoting prostate cancer aggressiveness.

HIP1 stabilizes FGFR-4 and promotes sustained activation after ligand stimulation

To determine the biochemical and biological effects of HIP1 on FGF signaling and FGFR-4 we established cells lines from the immortalized normal prostate cell line PNT1A and LNCaP prostate cancer cells expressing HIP1 under a constitutive promoter. As can be seen in Fig 3A, for both types of cells, expression of HIP1 in a clone was associated with markedly increased FGFR-4 protein levels. Quantitative RT-PCR to determine FGFR-4 receptor mRNA expression levels revealed no increase, and in most cases, slight decreases in FGFR-4 mRNA levels (Fig 3B). Thus HIP1 increases FGFR-4 protein via a post-transcriptional mechanism. To determine if this was due to altered receptor stability, we cotransfected 293T cells with either FGFR-4 variant and HIP1 expression constructs. We evaluated receptor stability of biotin labeled surface receptors at intervals following ligand stimulation followed by precipitation of biotin labeled proteins from cell lysates using streptavidin beads followed by Western blotting with anti-V5 antibody recognizing a V-5 tag on the transfected FGFR-4 variants (as in Fig 1A). We have found that HIP1 appears to specifically increase stability of the FGFR-4 Gly³⁸⁸ variant (Fig 4A). Note that both PNT1A and LNCaP cells have an Arg³⁸⁸/Gly³⁸⁸ genotype so that the effects seen in 293T cells are consistent with the results seen in the stable cell lines from these cells (Fig 3). To determine if this was accompanied by sustained receptor phosphorylation, we cotransfected 293T cells with either FGFR-4 variant and HIP1 and collected cell lysates at intervals after ligand stimulation. Total FGFR-4 was then immunoprecipitated with anti-V5 antibody and tyrosine phosphorylated FGFR-4 detected by Western blot. As shown in Figure 4B, expression of HIP1 resulted in sustained tyrosine phosphorylation of FGFR-4 Gly³⁸⁸ variant, but did not further increase phosphorylation of the Arg³⁸⁸ variant.

HIP1 interacts directly with FGFR-4

We next carried out reciprocal IP-Western blot studies to determine if there is a direct interaction between the FGFR-4 variants and HIP1. V5 tagged FGFR-4 and Flag-tagged HIP1 were cotransfected into 293T cells. Immunoprecipitation with anti-V5 antibody followed by Western blot with anti-Flag antibody (or the converse) revealed direct interaction between both FGFR-4 variant and HIP1, including an N-terminal truncated HIP1 (Fig 5A). Similar results were seen in prostate cancer cell lines (LAPC4 and LNCaP, data not shown). To map the domains of HIP1 that mediate the interaction with FGFR-4 we made a series of HIP1 deletion constructs (Fig 5B) that were then expressed in bacteria and proteins purified using streptavidin beads (Fig 5C). We then incubated the purified HIP1 proteins with lysates from 293T cells transfected with V5-tagged overnight and immunoprecipitated with streptavidin beads. The beads were washed and Western blots performed using an anti-V5 antibody. As shown in Fig 5D, the region between amino acids 601-798 containing the coiled-coil domain of HIP1 is required for HIP1-FGFR-4 interaction.

HIP1 potentiates the biological activities of FGFR-4

We next examined the biological affects of increased HIP1 expression. Cell lines expressing 2- to 5-fold higher levels of HIP1 were established by stable transfection (Fig 6A). In both PNT1A and DU145 prostate cancer cells, increased expression of full length HIP1 increases proliferation in media containing FGF2 and insulin as the only growth factors (Fig 6B). This effect was not seen with a truncated receptor that lacks the lipid binding domain of HIP1, which is required for its membrane localization in cells (27). It should be noted that DU145 cells are homozygous for the Gly³⁸⁸ allele while PNT1A cells are heterozygous Gly³⁸⁸/Arg³⁸⁸. The HIP1 overexpressing PNT1A cells were then infected with lentivirus expressing SjRNA targeting HIP1 or FGFR-4. As can be seen in Fig 6C, knockdown of FGFR-4 decreases growth of HIP1 overexpressing cells below that of control PNT1A in defined medium with FGF2 and insulin as the only growth factors. Thus, FGFR-4 is a major contributor to HIP1 induced growth in

response to FGFs in prostate epithelial cells. Similar increases in proliferation in PNT1A cells expressing HIP1 were seen in serum-containing medium that was significantly decreased by downregulation of FGFR-4 with siRNA (Fig 6C). These results imply that, even in complex media containing a variety of growth factors, FGFR-4 is a major effector of HIP1-mediated proliferation. Similar increases in proliferation in HIP1 overexpressing PNT1A cells were seen in media containing only 0.5% serum (data not shown). PNT1A cells are immortalized but not fully transformed and do not form colonies in soft agar. Expression of HIP1 leads to colony formation in soft agar (Fig 6D). Downregulation of FGFR-4 by 50% with siRNA partially abolishes this phenotype, (HIP1 Vs HIP1 FiSiR4, p=0.03), again implying that FGFR-4 plays a role in mediating HIP1 effects even in serum-containing medium. It should be noted that downregulation of HIP-1 by SiRNA resulted in even more marked decreases in proliferation and colony formation (Fig 6B and 6C), implying other receptors may also contribute to the phenotype induced by HIP1 overexpression.

DISCUSSION

We have shown previously in a large study of men with clinically localized prostate cancer that heterozygosity of the FGFR-4 Arg³⁸⁸ was associated with increased risk of pelvic lymph node metastasis at the time of radical prostatectomy and increased risk of biochemical recurrence (13). Heterozygosity of the FGFR-4 Arg³⁸⁸ has been associated with aggressive disease and clinical progression in a variety of other malignancies as well (16-21). Our prior *in vitro* studies have shown that expression of the FGFR-4 Arg³⁸⁸ allele results in increased motility and invasion. Of note, recent studies by Sahadevan et al (15) have shown that knockdown of FGFR-4 in PC3 cells (homozygous for Arg³⁸⁸) decreases proliferation and invasion *in vitro*. Thus it is clear that the FGFR-4 Arg³⁸⁸ allele can promote prostate cancer progression and is more effective than the Gly³⁸⁸ allele in this regard. However, FGFR-4 Gly³⁸⁸ may also promote progression since Sahadevan et al (15) have shown that knockdown of FGFR-4 in DU145,

which are homozygous for the Gly³⁸⁸ allele, can decrease proliferation and invasion of these cells *in vitro*. We have found that DU145 cells express basal levels of HIP1 (data not show), which may be enhancing the biological activity of the FGFR-4 Gly³⁸⁸ allele in these cells.

Our current data indicates that the FGFR-4 Arg³⁸⁸ variant has increased receptor stability and sustained phosphorylation which probably explains its ability to promote prostate cancer initiation and progression. FGFR-4 associates with HIP1 and the Gly³⁸⁸ variant is significantly stabilized by this interaction and results in phenotypes associated with cancer, including increased proliferation in low growth factor conditions and colony formation in soft agar. The decreased receptor degradation and sustained phosphorylation after ligand stimulation that we observed may substantially amplify receptor signaling by increasing surface receptor concentrations and local FGF ligand (by decreasing degradation) and by increasing the pool of early endosomes with bound ligand, which can continue to transduce signals (27). Further studies, including direct comparison of the FGFR-4 Arg³⁸⁸ and Gly³⁸⁸ alleles and with other FGF receptors, are needed to understand the molecular basis of the increased receptor stability and sustained phosphorylation after ligand stimulation observed with the FGFR-4 Arg³⁸⁸ variant.

We have also demonstrated that the FGFR-4 Gly³⁸⁸ variant is stabilized after ligand stimulation by the presence of HIP1. This may be mediated through a direct interaction via the coiled-coil domain located between amino acids 601-798. Of note, a recent study by Bradley et al (31) have shown a similar direct interaction between HIP1 and EGF receptor which requires a domain between amino acids 381-814 of HIP1. In addition, it has been shown that amino acids 690-752 of HIP1 are required for transformation by the HIP1/PDGR-beta fusion gene (32). Thus the domain we have identified overlaps with the regions identified for direct interaction of HIP1 with EGF receptors, although it is not clear that the interacting domains are the same. Previous studies have indicated that HIP1 alters clathrin-mediated membrane trafficking of EGF receptors (27, 28), so it is likely that it also has a similar affect on FGFR-4 Gly³⁸⁸, although other

mechanisms are possible as well. Interestingly, HIP1 did not further increase Arg³⁸⁸ stability, perhaps because this variant is already extremely stable after ligand stimulation. Further mechanistic studies are needed to determine the molecular basis by which HIP1 stabilizes the FGFR-4 Gly³⁸⁸ but not the Arg³⁸⁸ variant.

Prior work by Rao et al (28) has shown that HIP1 can strongly enhance EGF receptor signaling, with potent biological effects in NIH3T3 cells. We have demonstrated that HIP1 has similar potent effects in prostate and prostate cancer cell lines that are mediated in part via FGFR-4, even in culture media containing serum, which is a poor source of FGFs. Given the high local concentrations of FGF2 in tumors *in vivo* (6) and the prevalent expression of other FGFR-4 binding FGF ligands as autocrine factors (5, 8-11), it is likely that FGFR-4 plays an even more important role in mediating the effects of HIP1 in human cancers *in vivo*. Other growth factor receptors, including other FGF receptor family members as well as EGF receptor family members, may well contribute to the biological activities of HIP1 in prostate cancer. Rao et al (28) noted that HIP1 increases the level of FGFR-4 (and FGFR-3) protein in NIH3T3 cells and hypothesized that these growth factor receptors may contribute to the phenotype in HIP1 expressing NIH3T3 cells, although their data indicated that EGF receptors probably played a dominant role in these cells. Thus the relative importance of different receptors in mediating the phenotypes in cells expressing HIP1 may be cell type specific.

Based on the results reported here and by others, altered FGFR-4 stability and/or trafficking is extremely common in prostate cancer. Our prior studies have shown that more than half of all white men with prostate cancer are hetero- or homozygous for the FGFR-4 Arg³⁸⁸ allele (13) and immunohistochemical studies have shown that almost all prostate cancers express FGFR-4 (13-15). Furthermore, approximately 50% of clinically localized prostate cancers express moderate to strong levels of HIP1 (29), and presumably the expression of HIP1 is independent of the FGFR-4 genotype, although there might be selection for HIP1 expression in prostate cancers homozygous for the Gly³⁸⁸ variant. If these two factors are independent, it is

likely that at least 75% of prostate cancers have alterations of FGFR-4 signaling via receptor stabilization and, based on our studies and those of others, this altered signaling has important biological and clinical consequences. Thus enhanced FGFR-4 signaling is one of the most common alterations in human prostate cancer. FGFR-4 is therefore an important therapeutic target in prostate cancer and development of such therapies should be pursued vigorously.

REFERENCES

1. Jemal A, Siegel R, Ward E, Murray T, Xu J, Thun MJ. Cancer statistics, 2007. CA Cancer J Clin 2007;57(1):43-66.
2. Kwabi-Addo B, Ozen M, Ittmann M. The role of fibroblast growth factors and their receptors in prostate cancer. Endocr Relat Cancer 2004;11(4):709-24.
3. Powers CJ, McLeskey SW, Wellstein A. Fibroblast growth factors, their receptors and signaling. Endocr Relat Cancer 2000;7(3):165-97.
4. Ozen M, Giri D, Ropiquet F, Mansukhani A, Ittmann M. Role of fibroblast growth factor receptor signaling in prostate cancer cell survival. J Natl Cancer Inst 2001;93(23):1783-90.
5. Dorkin TJ, Robinson MC, Marsh C, Neal DE, Leung HY. aFGF immunoreactivity in prostate cancer and its co-localization with bFGF and FGF8. J Pathol 1999;189(4):564-9.
6. Giri D, Ropiquet F, Ittmann M. Alterations in expression of basic fibroblast growth factor (FGF) 2 and its receptor FGFR-1 in human prostate cancer. Clin Cancer Res 1999;5(5):1063-71.
7. Gravdal K, Halvorsen OJ, Haukaas SA, Akslen LA. Expression of bFGF/FGFR-1 and vascular proliferation related to clinicopathologic features and tumor progress in localized prostate cancer. Virchows Arch 2006;448(1):68-74.
8. Ropiquet F, Giri D, Kwabi-Addo B, Mansukhani A, Ittmann M. Increased expression of fibroblast growth factor 6 in human prostatic intraepithelial neoplasia and prostate cancer. Cancer Res 2000;60(15):4245-50.
9. Dorkin TJ, Robinson MC, Marsh C, Bjartell A, Neal DE, Leung HY. FGF8 over-expression in prostate cancer is associated with decreased patient survival and persists in androgen independent disease. Oncogene 1999;18(17):2755-61.
10. West AF, O'Donnell M, Charlton RG, Neal DE, Leung HY. Correlation of vascular endothelial growth factor expression with fibroblast growth factor-8 expression and clinico-pathologic parameters in human prostate cancer. Br J Cancer 2001;85(4):576-83.
11. Heer R, Douglas D, Mathers ME, Robson CN, Leung HY. Fibroblast growth factor 17 is over-expressed in human prostate cancer. J Pathol 2004;204(5):578-86.
12. Eswarakumar VP, Lax I, Schlessinger J. Cellular signaling by fibroblast growth factor receptors. Cytokine Growth Factor Rev 2005;16(2):139-49.
13. Wang J, Stockton DW, Ittmann M. The fibroblast growth factor receptor-4 Arg388 allele is associated with prostate cancer initiation and progression. Clin Cancer Res 2004;10(18 Pt 1):6169-78.
14. Gowardhan B, Douglas DA, Mathers ME, *et al.* Evaluation of the fibroblast growth factor system as a potential target for therapy in human prostate cancer. Br J Cancer 2005;92(2):320-7.
15. Sahadevan K, Darby S, Leung H, Mathers M, Robson C, Gnanapragasam V. Selective over-expression of fibroblast growth factor receptors 1 and 4 in clinical prostate cancer. J Pathol 2007;213(1):82-90.
16. Bange J, Prechtel D, Cheburkin Y, *et al.* Cancer progression and tumor cell motility are associated with the FGFR4 Arg(388) allele. Cancer Res 2002;62(3):840-7.
17. Morimoto Y, Ozaki T, Ouchida M, *et al.* Single nucleotide polymorphism in fibroblast growth factor receptor 4 at codon 388 is associated with prognosis in high-grade soft tissue sarcoma. Cancer 2003;98(10):2245-50.

18. Streit S, Mestel DS, Schmidt M, Ullrich A, Berking C. FGFR4 Arg388 allele correlates with tumour thickness and FGFR4 protein expression with survival of melanoma patients. *Br J Cancer* 2006;94(12):1879-86.
19. Spinola M, Leoni V, Pignatiello C, *et al.* Functional FGFR4 Gly388Arg polymorphism predicts prognosis in lung adenocarcinoma patients. *J Clin Oncol* 2005;23(29):7307-11.
20. Streit S, Bange J, Fichtner A, Ihrler S, Issing W, Ullrich A. Involvement of the FGFR4 Arg388 allele in head and neck squamous cell carcinoma. *Int J Cancer* 2004;111(2):213-7.
21. da Costa Andrade VC, Parise O, Jr., Hors CP, de Melo Martins PC, Silva AP, Garicochea B. The fibroblast growth factor receptor 4 (FGFR4) Arg388 allele correlates with survival in head and neck squamous cell carcinoma. *Exp Mol Pathol* 2007;82(1):53-7.
22. Jezequel P, Campion L, Joalland MP, *et al.* G388R mutation of the FGFR4 gene is not relevant to breast cancer prognosis. *Br J Cancer* 2004;90(1):189-93.
23. Thussbas C, Nahrig J, Streit S, *et al.* FGFR4 Arg388 allele is associated with resistance to adjuvant therapy in primary breast cancer. *J Clin Oncol* 2006;24(23):3747-55.
24. Wang J, Cai Y, Penland R, Chauhan S, Miesfeld RL, Ittmann M. Increased expression of the metastasis-associated gene Ehm2 in prostate cancer. *Prostate* 2006;66(15):1641-52.
25. Monsonego-Ornan E, Adar R, Feferman T, Segev O, Yayon A. The transmembrane mutation G380R in fibroblast growth factor receptor 3 uncouples ligand-mediated receptor activation from down-regulation. *Mol Cell Biol* 2000;20(2):516-22.
26. Cho JY, Guo C, Torello M, *et al.* Defective lysosomal targeting of activated fibroblast growth factor receptor 3 in achondroplasia. *Proc Natl Acad Sci U S A* 2004;101(2):609-14.
27. Hyun TS, Rao DS, Saint-Dic D, *et al.* HIP1 and HIP1r stabilize receptor tyrosine kinases and bind 3-phosphoinositides via epsin N-terminal homology domains. *J Biol Chem* 2004;279(14):14294-306.
28. Rao DS, Bradley SV, Kumar PD, *et al.* Altered receptor trafficking in Huntington Interacting Protein 1-transformed cells. *Cancer Cell* 2003;3(5):471-82.
29. Rao DS, Hyun TS, Kumar PD, *et al.* Huntington-interacting protein 1 is overexpressed in prostate and colon cancer and is critical for cellular survival. *J Clin Invest* 2002;110(3):351-60.
30. Wang J, Cai Y, Ren C, Ittmann M. Expression of Variant TMPRSS2/ERG Fusion Messenger RNAs Is Associated with Aggressive Prostate Cancer. *Cancer Res* 2006;66(17):8347-51.
31. Bradley SV, Holland EC, Liu GY, Thomas D, Hyun TS, Ross TS. Huntington interacting protein 1 is a novel brain tumor marker that associates with epidermal growth factor receptor. *Cancer Res* 2007;67(8):3609-15.
32. Ross TS, Gilliland DG. Transforming properties of the Huntington interacting protein 1/ platelet-derived growth factor beta receptor fusion protein. *J Biol Chem* 1999;274(32):22328-36.

FIGURE LEGENDS

Figure 1. Stabilization and sustained activation of the FGFR-4 Arg³⁸⁸ variant.

A. 293T cells were transfected with V5 –tagged FGFR-4 Arg³⁸⁸ or Gly³⁸⁸ and cell surface receptors labeled with biotin. Cells were then stimulated with FGF2 and lysed at the indicated time. Labeled receptors were then immunoprecipitated with streptavidin-agarose and FGFR-4 detected by Western blot of the immunoprecipitates with anti-V5 antibody. Western blot of an aliquot of the lysate used for immunoprecipitation with anti-β-actin antibody is shown. B. 293T cells were transfected with either V5-tagged FGFR-4 Arg³⁸⁸ or Gly³⁸⁸. After overnight incubation in media with insulin as the only growth factor, cells were stimulated with FGF2 for the indicated number of minutes and lysates prepared. Tagged FGFR-4 was immunoprecipitated with ant-V5 antibody and phosphorylated receptor detected by Western blot of immunoprecipitates with anti-phosphotyrosine antibody. Western blot with anti-V5 antibody is shown to confirm equivalent immunoprecipitation. C. Experiment similar to B except with longer intervals of FGF2 treatment. Western blot was carried out with anti-V5 antibody to confirm equal amounts of FGFR-4. In addition, Western blot of an aliquot of the lysate used for immunoprecipitation with anti-β-actin antibody was performed.

Figure 2. Quantitation of HIP1 transcripts by quantitative RT-PCR in prostate cancer.

Quantitative RT-PCR was performed on RNAs extracted from benign peripheral zone tissue from radical prostatectomies (PZ) or prostate cancers from patients with no PSA recurrence within 5 years of surgery (Non-recur) or with PSA recurrence within 5 years of surgery. β-actin transcript levels were used for normalization. Mean +/- standard deviation is shown.

Figure 3. Stabilization of FGFR-4 by HIP1 in prostate epithelial and prostate cancer cells.

Immortalized normal prostate epithelial cells (PNT1A) or prostate cancer cells (LNCaP) were transfected with HIP1 in the TOPO-V5 expression vector and stable cells lines selected. Expression of HIP1 and FGFR-4 protein was evaluated by Western blot with β-actin as a

loading control. Expression of FGFR-4 mRNA was determined by quantitative RT-PCR with normalization to β-actin transcript levels.

Figure 4. Stabilization of FGFR-4 Gly³⁸⁸ by HIP1

A. 293T cells were transfected with V5 –tagged FGFR-4 Arg³⁸⁸ or Gly³⁸⁸ with or without HIP1 and cell surface receptors labeled with biotin. Cells were then stimulated with FGF2 and lysed at the indicated time. Labeled receptors were then immunoprecipitated with streptavidin-agarose and FGFR-4 detected by Western blot of the immunoprecipitates with anti-V5 antibody.

B. 293T cells were transfected with either V5-tagged FGFR-4 Arg³⁸⁸ or Gly³⁸⁸. After overnight incubation in media with insulin as the only growth factor, cells were stimulated with FGF2 for the indicated number of minutes and lysates prepared. Tagged FGFR-4 was immunoprecipitated with ant-V5 antibody and phosphorylated receptor detected by Western blot of immunoprecipitates with anti-phosphotyrosine antibody. Western blot with anti-V5 antibody is shown to confirm equivalent immunoprecipitation.

Figure 5. Direct interaction of FGFR-4 and HIP1

A. 293 T cells were transfected with Flag-tagged HIP1 or N-terminally truncated HIP 1 (-183) with or without either FGFR-4 Arg388 or Gly388 (both V5-tagged). Vector control (Tag2B) is also shown. Cell lysates were then analyzed by Western blot using anti-V5 or anti-Flag antibody or used for reciprocal immunoprecipitation and Western blotting with the two antibodies.

B. Map of HIP1 showing major domains and deletion fragments used to prepare bacterial fusion proteins. C. Purified HIP1 and HIP1 deletion bacterial fusion proteins on Coomassie Blue stained polyacrylamide gel following electrophoresis. D. 293T cells were transfected with V5-tagged FGFR-4 and lysates prepared and incubated with purified HIP1 and HIP1 deletion constructs. Complexes were then immunoprecipitated with streptavidin beads and Western blot performed with anti-V5 antibody. Control is streptavidin beads but no purified protein.

Figure 6. Biological affects of HIP1 in prostate and prostate cancer cell lines.

- A. Pooled prostate (PNT1A) or prostate cancer (DU145) cell lines expressing full length HIP1, an amino terminal truncated HIP1 or vector only were plated and growth determined in defined medium containing FGF2 and insulin as the only growth factors. Cell number was determined at two day interval. Mean +/- standard deviation of triplicates is shown.
- B. PNT1A cells overexpressing HIP1 were infected with lentivirus expressing ShRNA targeting HIP1 or FGFR-4 and stable expressors selected and pooled. Quantitative RT-PCR showed 70% and 60% knockdown of HIP1 and FGFR-4 mRNA, respectively (data not shown). Cells were then plated and grown in defined medium with FGF2 and insulin as the only growth factors or serum containing medium. Cell number was determined at two day intervals by cell counting. Mean +/- standard deviation of triplicates is shown.
- C. PNT1A cells as described in B) were plated in soft agar. Colony formation was evaluated by counting. Mean +/- standard deviation of triplicates is shown.

Figure 1

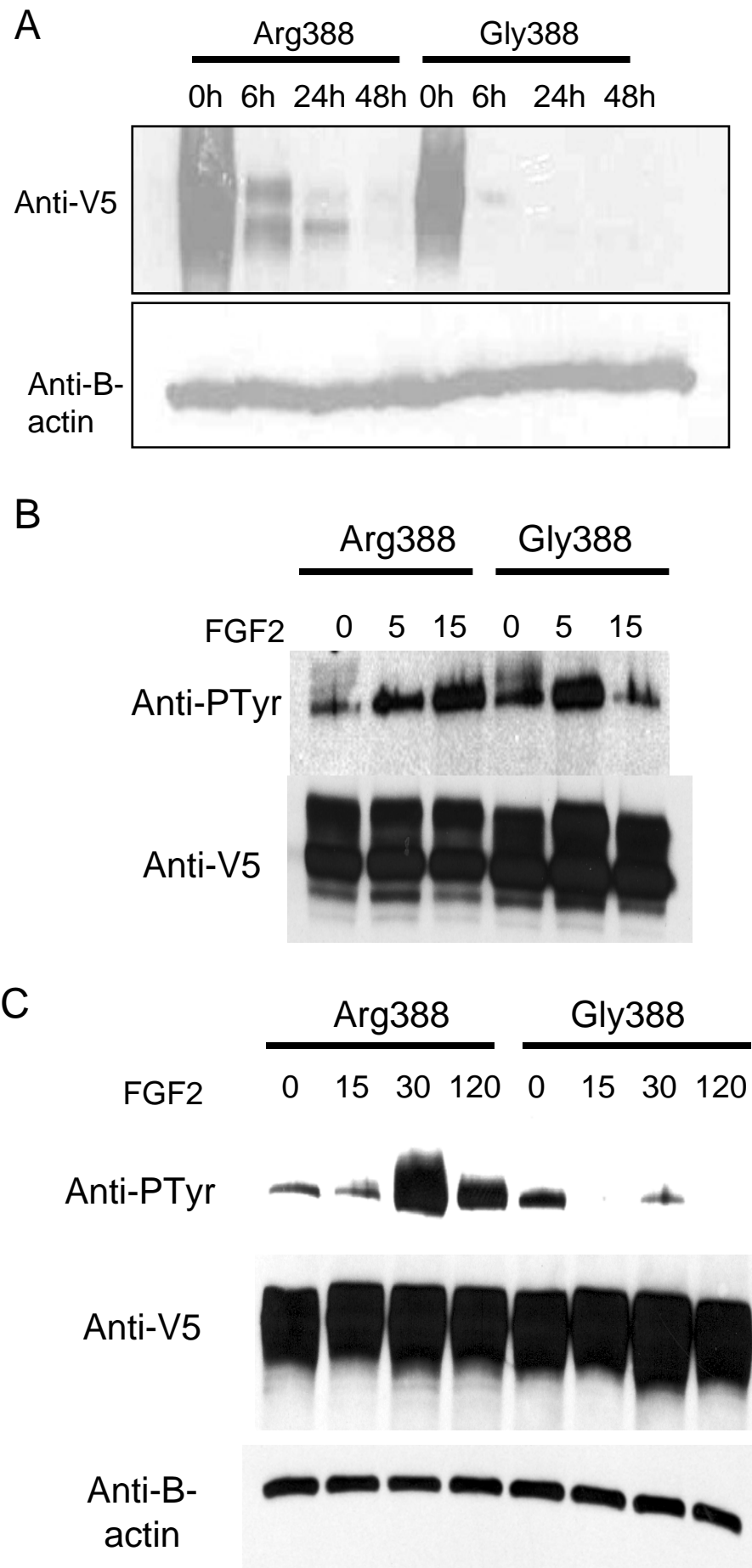


Figure 2.

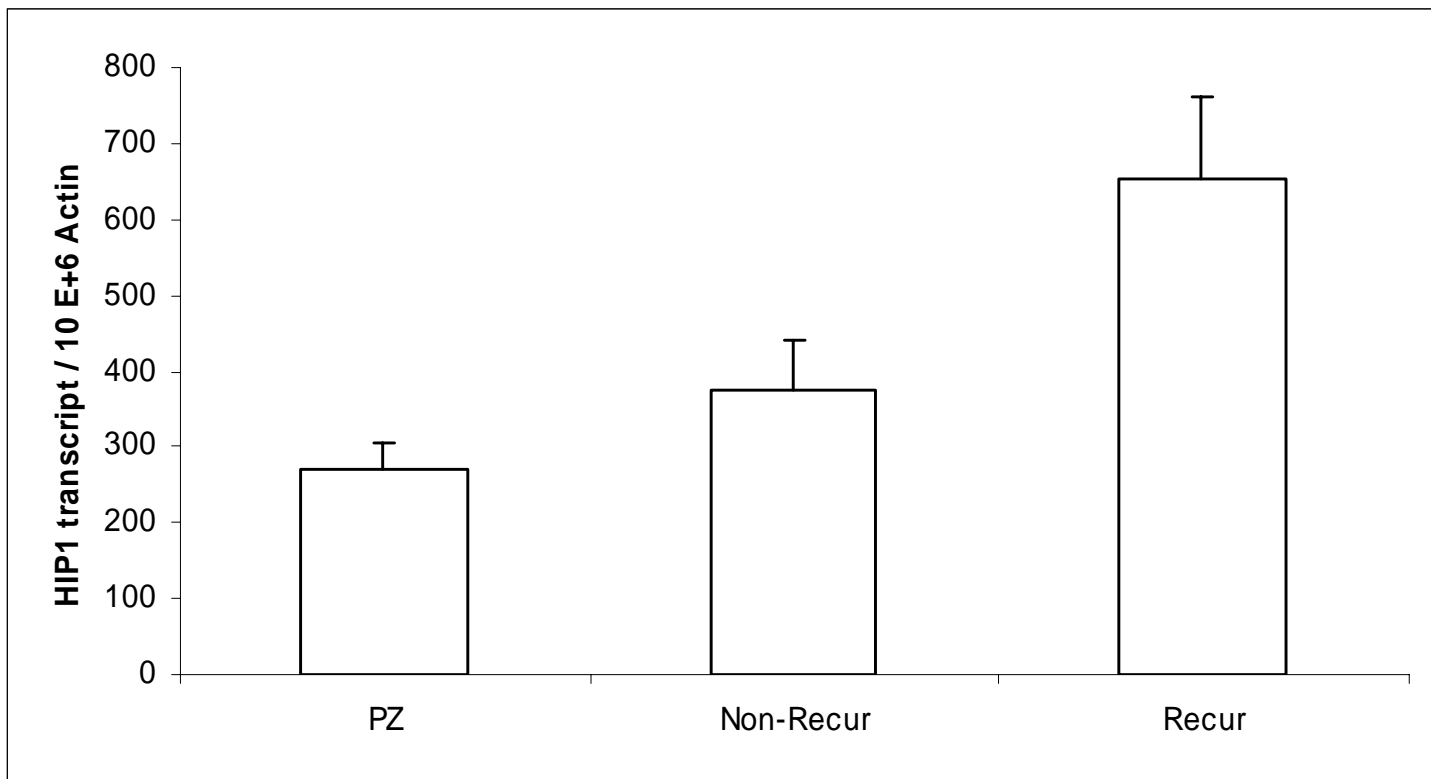
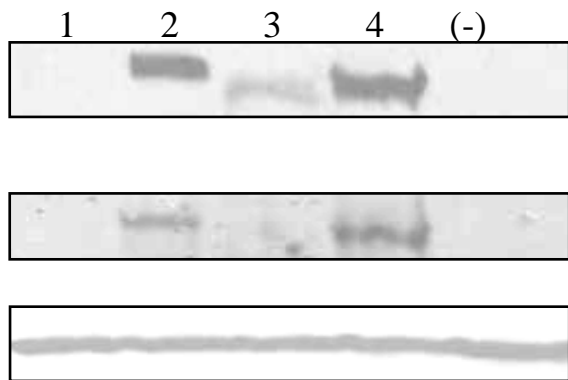
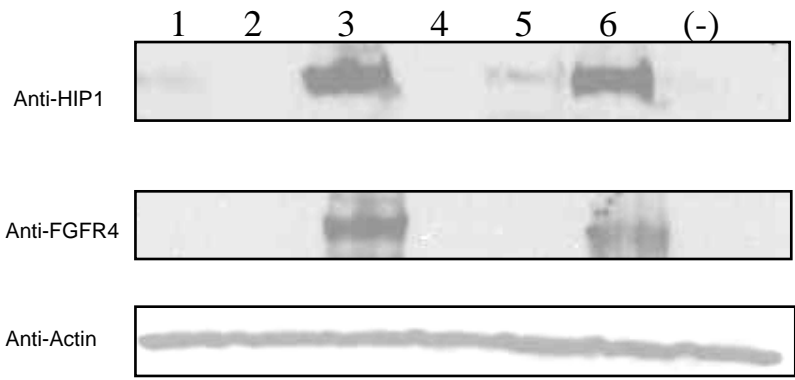


Figure 3

A

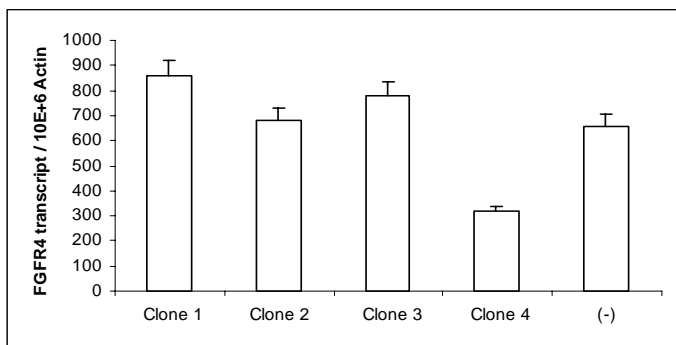


PNT1A HIP1 Clones

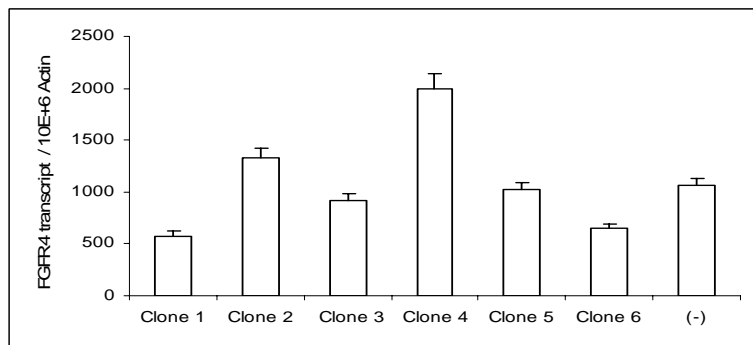


LNCaP HIP1 Clones

B



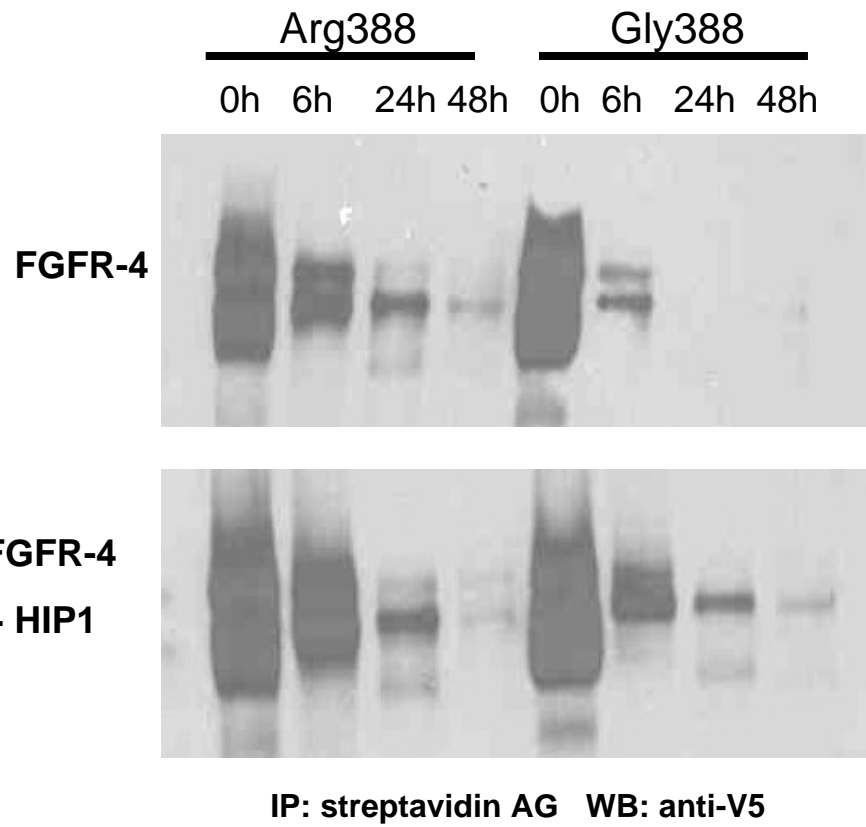
PNT1A HIP1 Clones



LNCaP HIP1 Clones

Figure 4

A



B

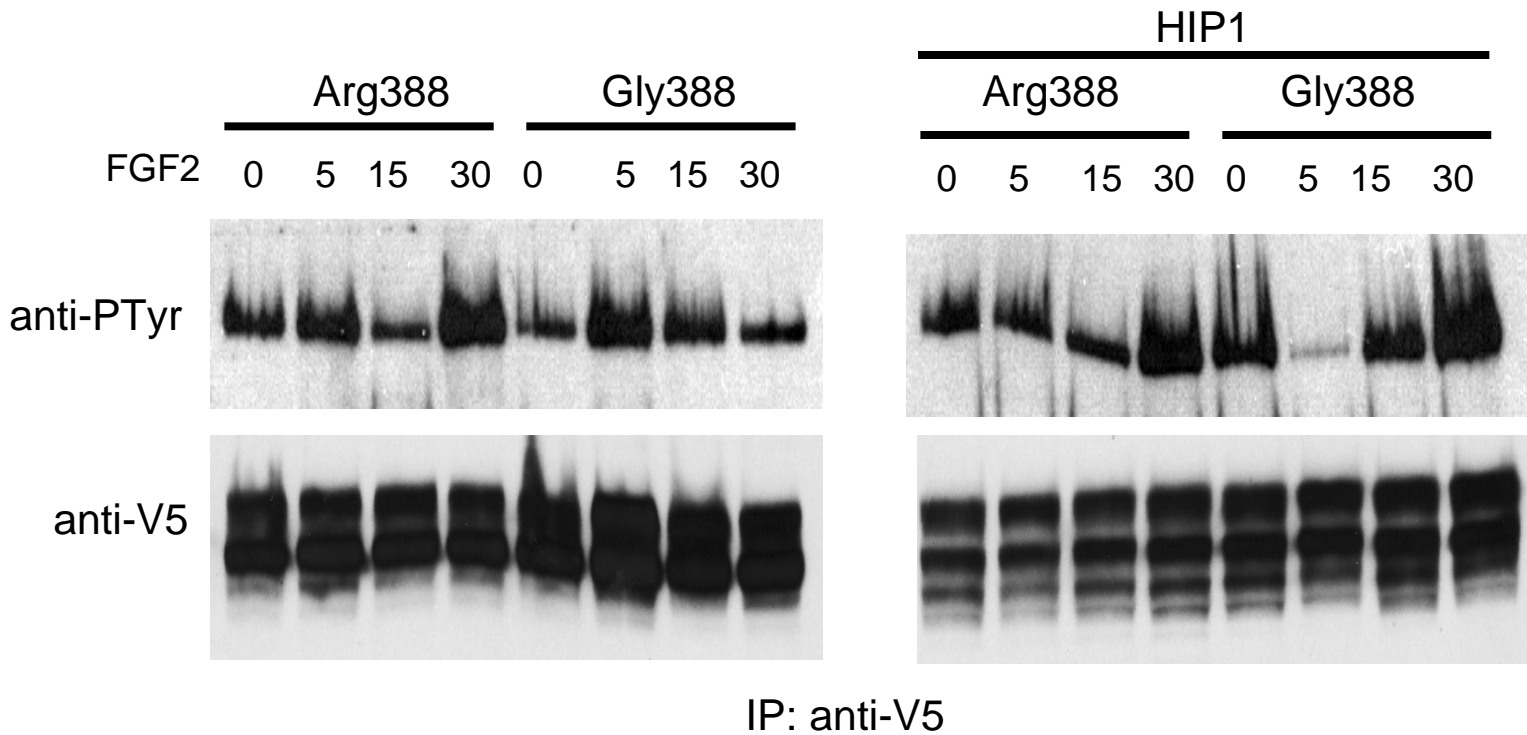
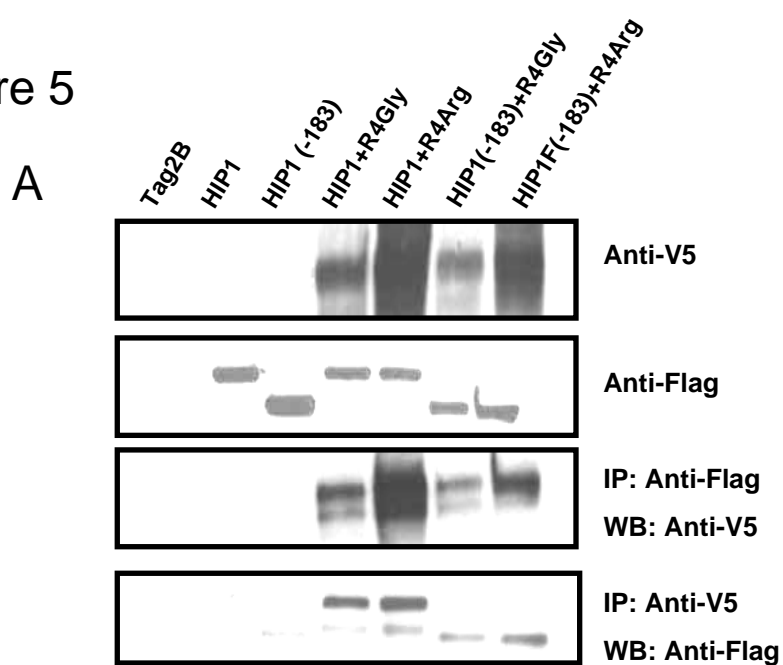
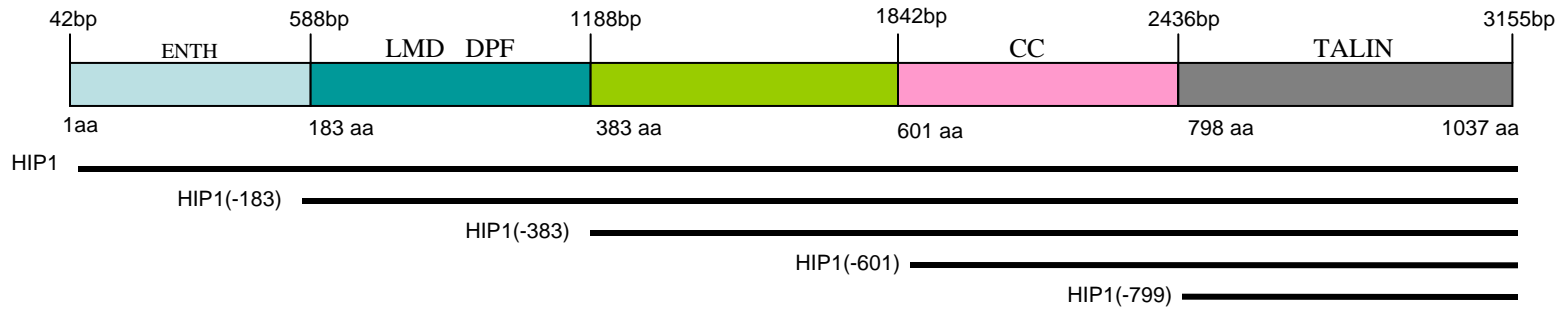


Figure 5



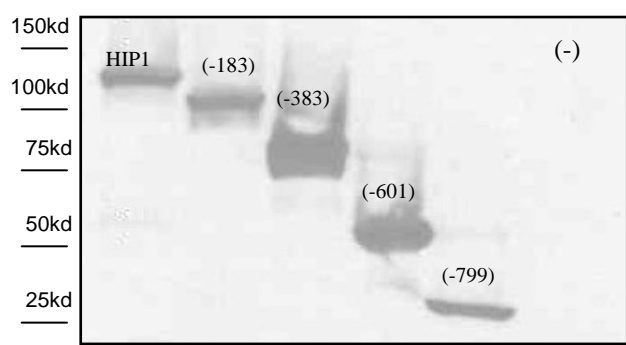
B



ENTH: Epsin N-terminal homology domain; LMD and DPF motifs can bind to clathrin and AP2;

CC: Central coiled coil domain C-terminal TALIN

C



D

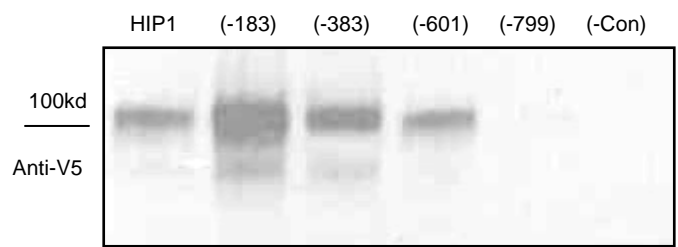
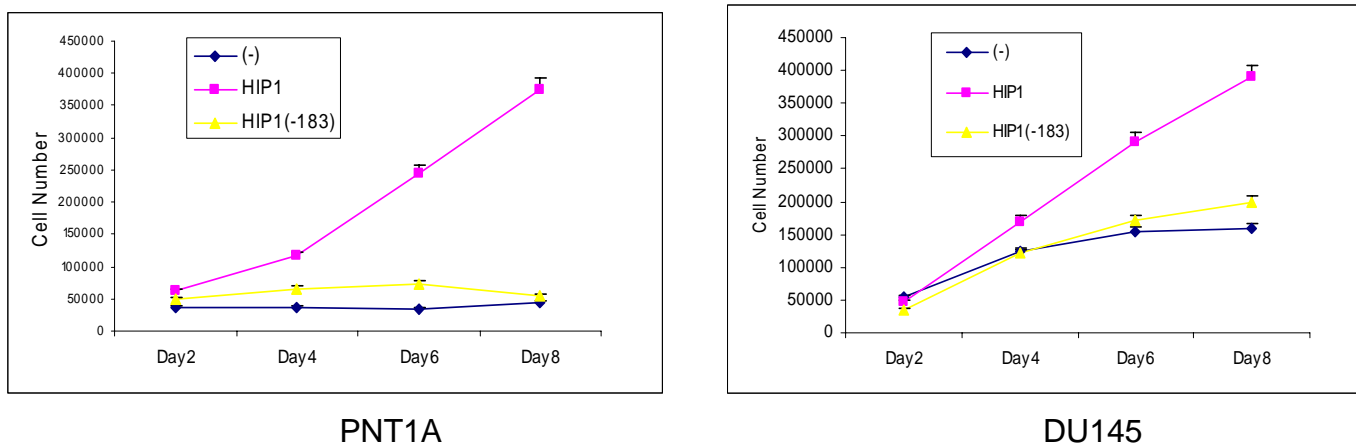


Figure 6

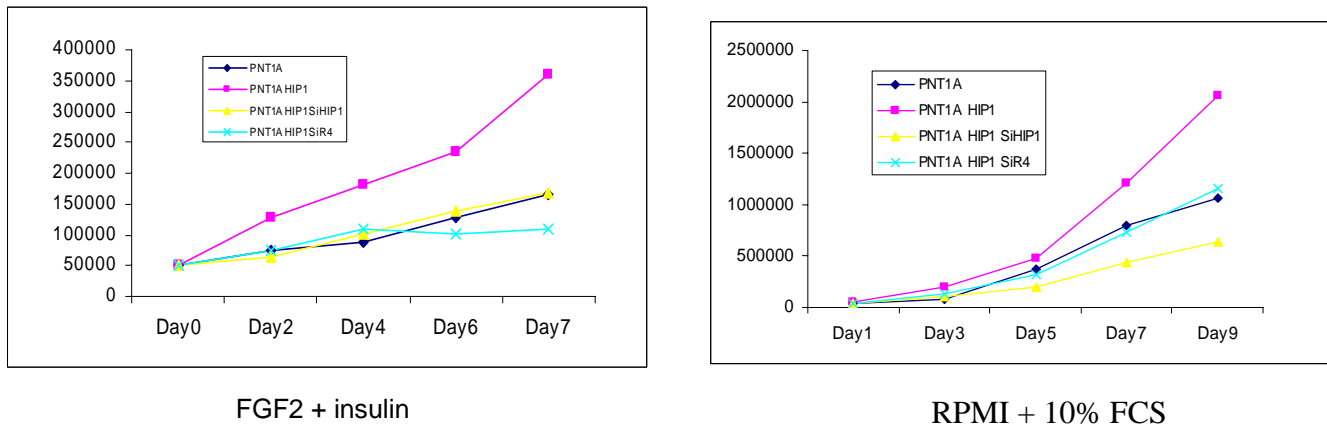
A.



PNT1A

DU145

B



FGF2 + insulin

RPMI + 10% FCS

C

